Vehicular Hydrogen Storage with ad(ab)sorbent Materials

Channing Ahn,
Caltech

Hydrogen and high end use

Shuttle launches with 100,000 kg of LH_2 alkaline fuel cell 65% efficiency for electricity.

<u>Aircraft</u> - high flame propagation speed high energy to wt ratio but low energy to vol.

X-43A (Mach 7-10) hydrogen-fueled.

<u>Boeing A2</u> on drawing board. Mach 5.5 (Concorde was Mach 2).

Planck Mission cryo-cooler

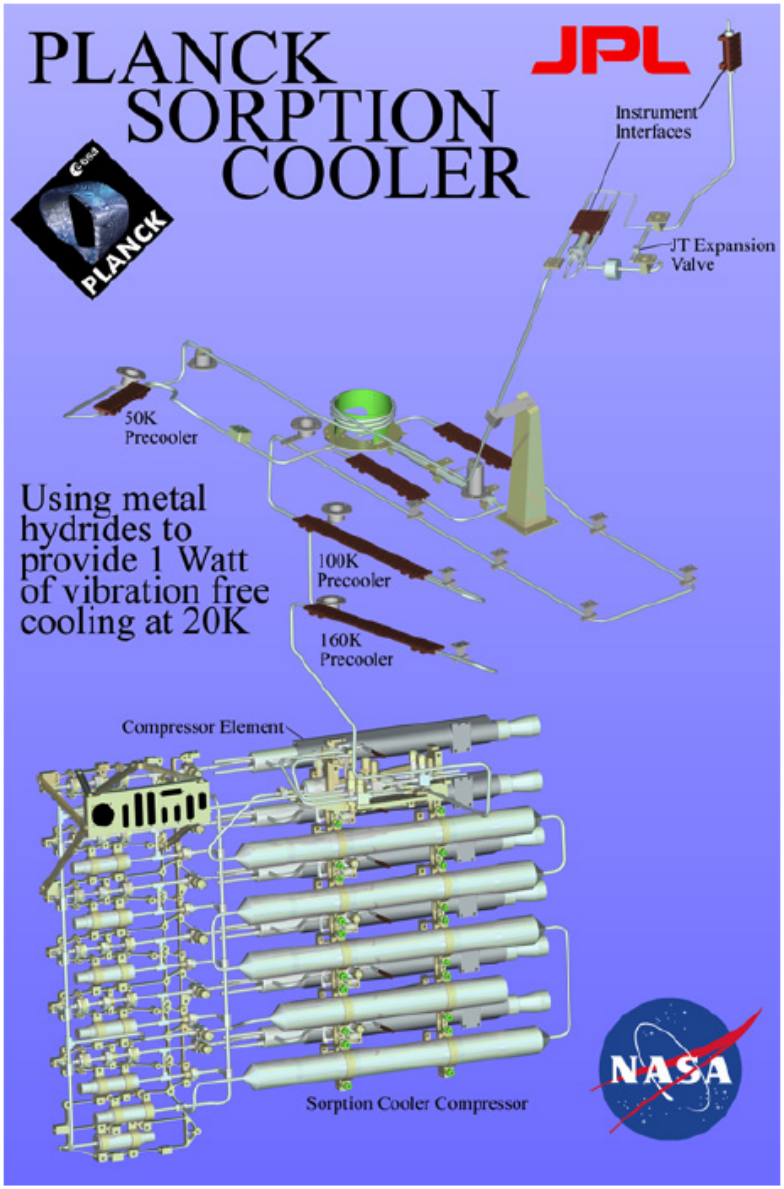

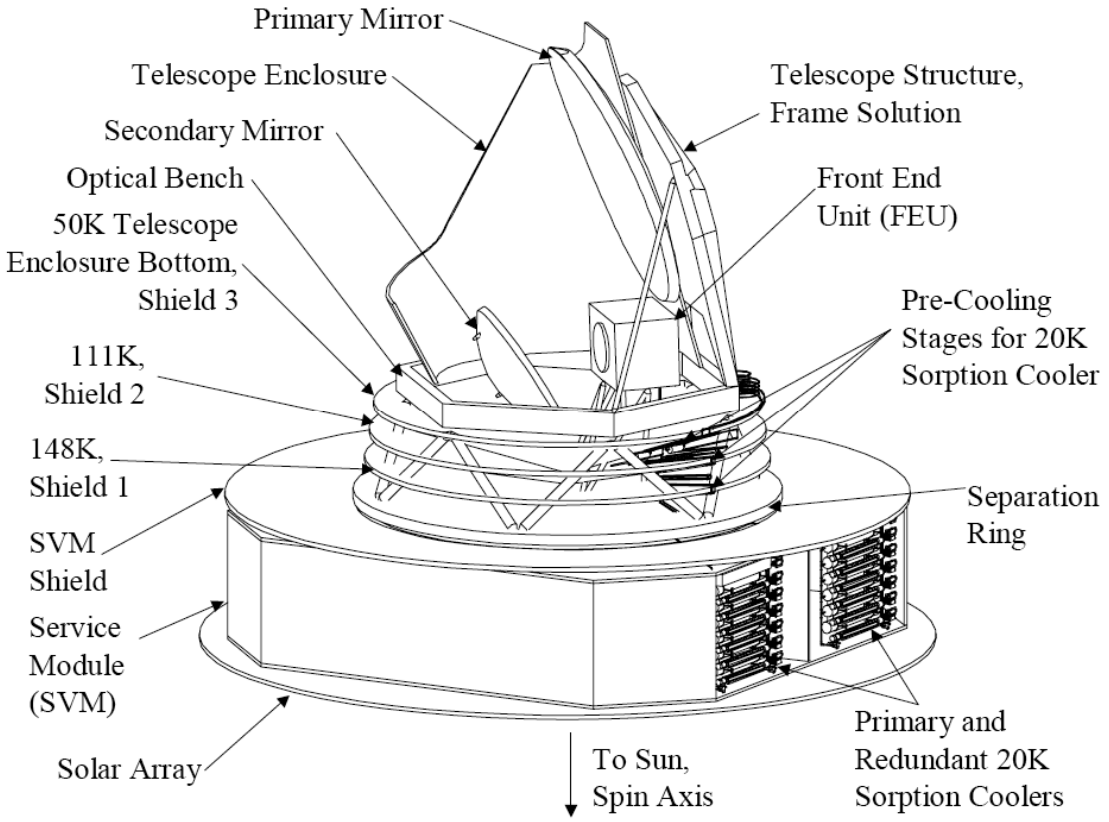

LaNiSn metal hydrides for use in sorbent beds of closed cycle Joule-Thomson device

R. C. Bowman, Jr.

Terrestrial mobile storage challenges

- Vehicles are being designed by OEMs that can achieve > 300 miles (500 km)
  - 350 or 700 bar
  - 1 to 4 tanks
  - Specified range from ~200 to > 350 miles
- But performance, space on-board and cost are still challenges for mass market penetration…
- Is there a low pressure alternative?

Courtesy G. Sandrock

Hydrogen Storage basics

Compressed Gas and Cryogenic Liquid Storage

Hydrogen can be physically stored as either a gas or a liquid. Storage as a gas typically requires high-pressure tanks (5000-10,000 psi tank pressure). Storage of hydrogen as a liquid requires cryogenic temperatures, since the boiling point of hydrogen at one atmosphere pressure is -252.8ºC.

Chemical hydrides also being studied but dehydrogenation exothermic so no onboard refueling with present systems.

Materials-based Hydrogen Storage

Hydrogen can also be stored on the surfaces of solids (by adsorption) or within solids (by absorption). In adsorption, hydrogen is attached to the surface of a material either as hydrogen molecules or as hydrogen atoms. In absorption, hydrogen is dissociated into H-atoms and then the hydrogen atoms are incorporated into the solid lattice framework.

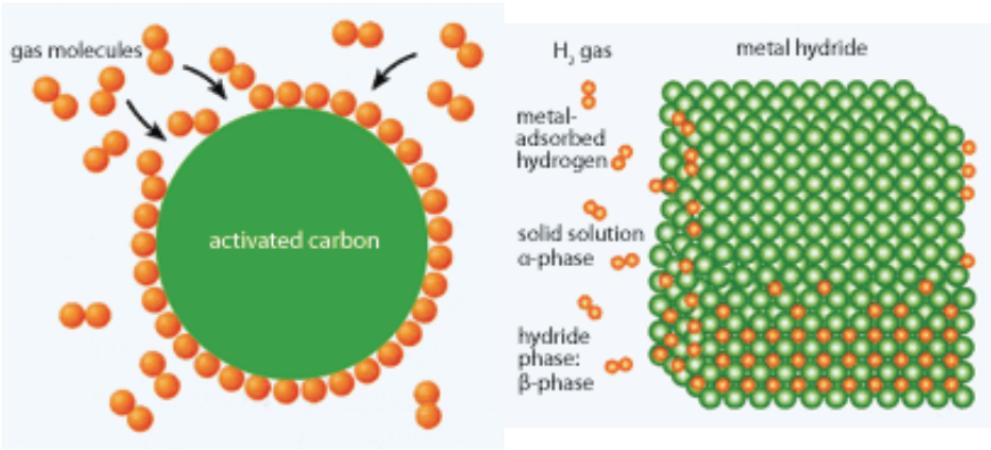

http://www.eere.energy.gov/

What about the real (vs ideal) gas law?

H_2 behavior at 77, 298 and 573K

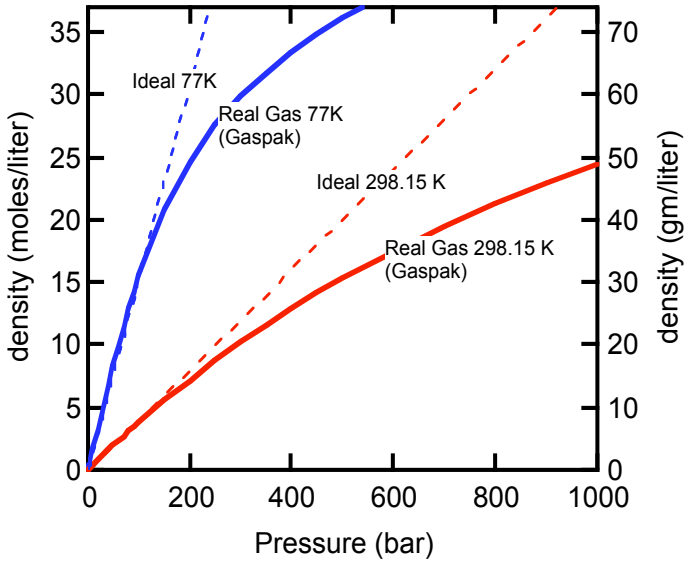

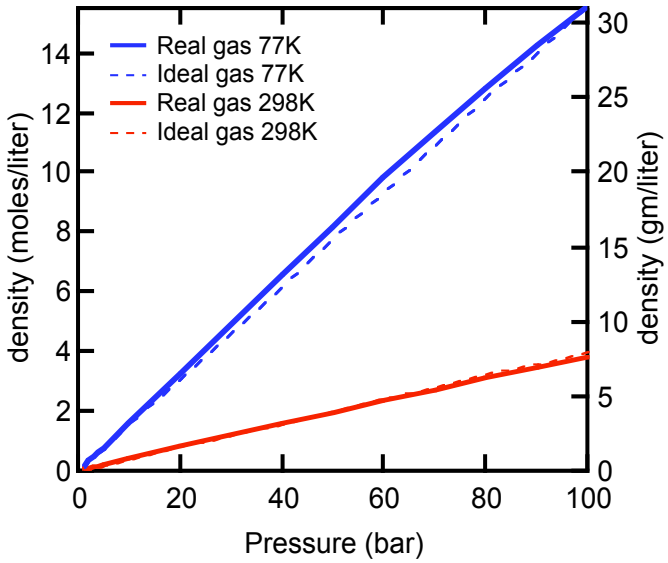

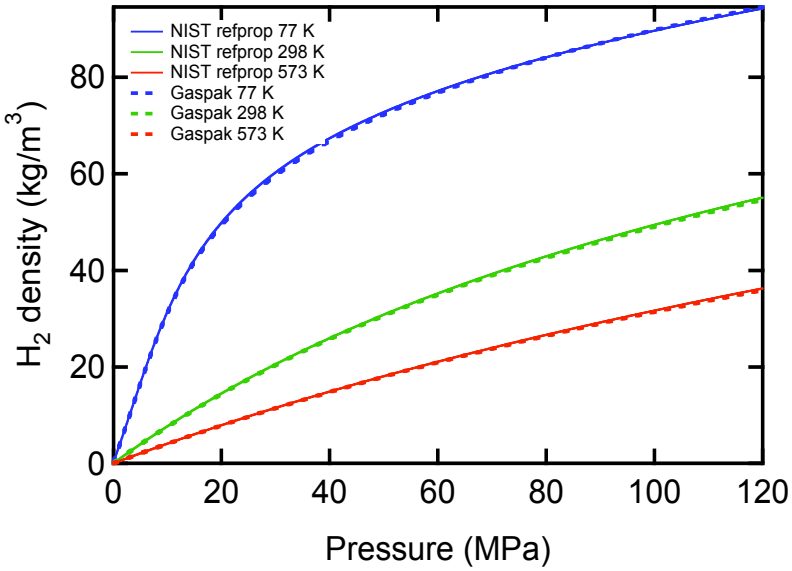

Comparison of Gaspak and Refprop at top.

Gaspak equations here updated from hydrogen properties from NBS Technical Monograph 168, February 1981, (R. D. McCarty, J. Hord and H. M. Roder). Equation of state valid from triple point to 5000 K, pressures to 1200 bar.

At pressures to 100 bar, real and ideal gas behavior similar for both 77K and RT

Heat generated for several reaction enthalpies

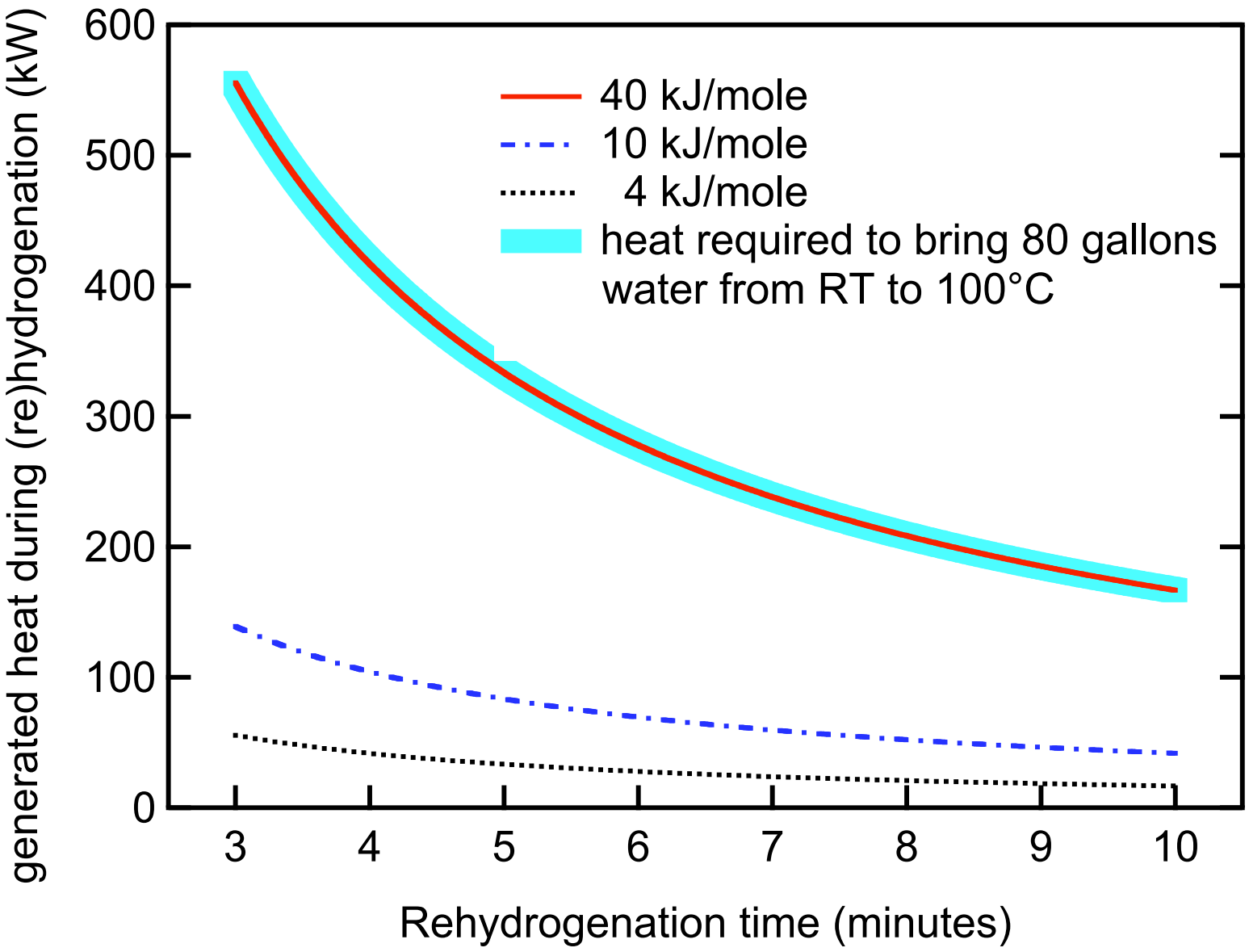

Its all about enthalpy (and a bit of entropy)!

What is the equilibrium pressure of H_2 in an adsorbent?

Functional form is the Langmuir isotherm.

$$bp = \frac{f}{1-f}$$

where, p = gas pressure and

$$b = \exp\left(\frac{\Delta\overline{H}}{RT} - \frac{s - s^0}{R}\right)$$

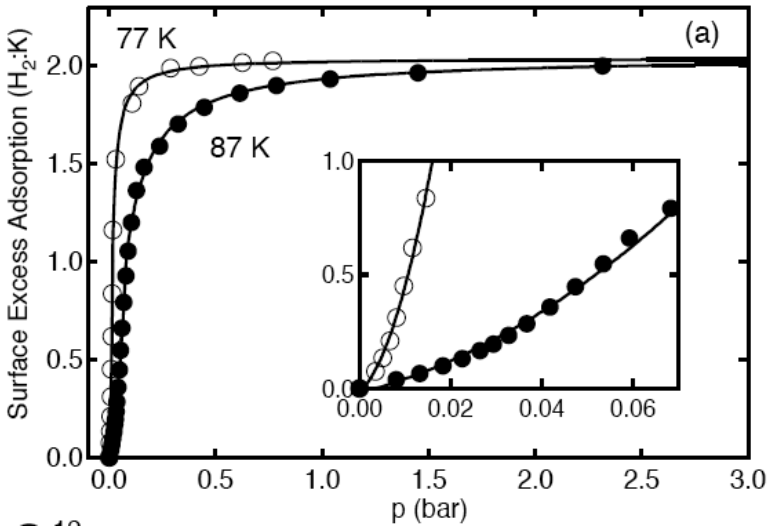

What is the equilibrium pressure of H_2 in an absorbent?

Functional form is the van't Hoff plot.

$$\ln P = \left(\frac{\Delta H}{RT} - \frac{\Delta S}{R}\right)$$

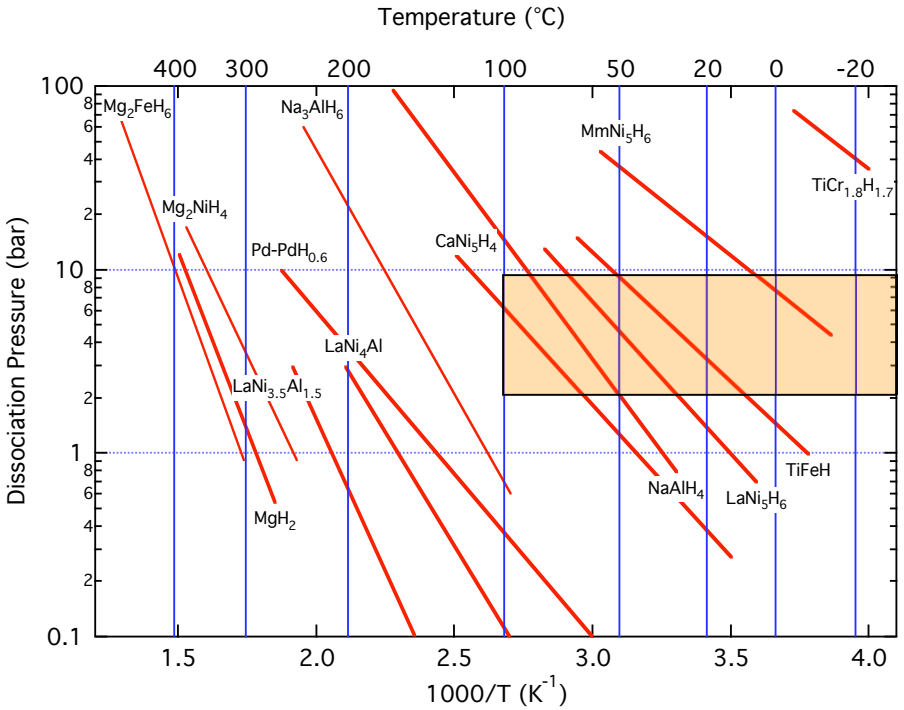

Porous solids and adsorption isotherms

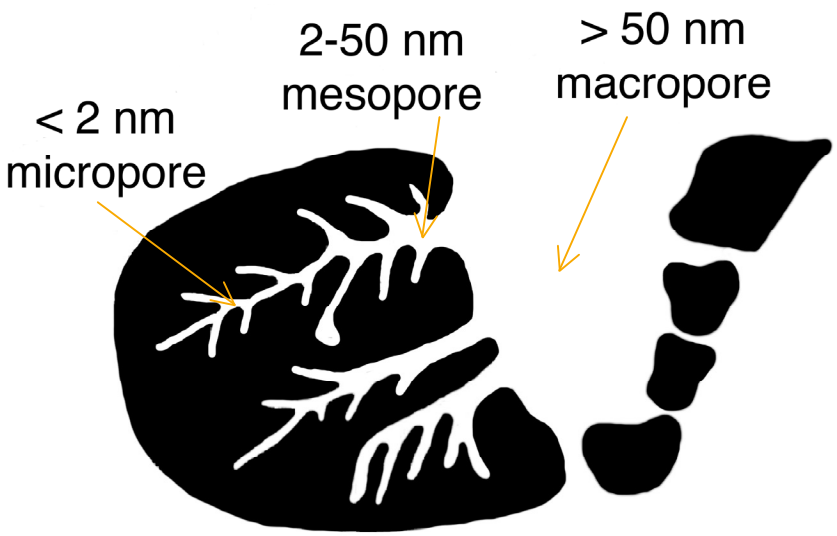

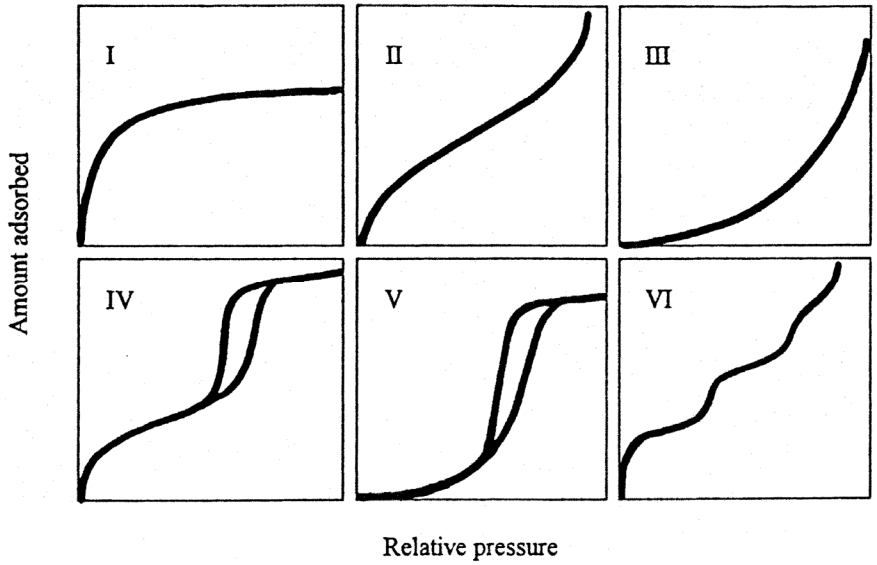

Langmuir (1916) recognized problems with describing sorption in charcoal

'it is impossible to know definitely the area on which the adsorption takes place,'

equations for planer sorption not applicable to 3d case.

IUPAC isotherm definitions above.

Micropore region of most relevance to hydrogen.

No multilayer phenomena expected.

Electron correlations weak.

Real isotherms and dependencies

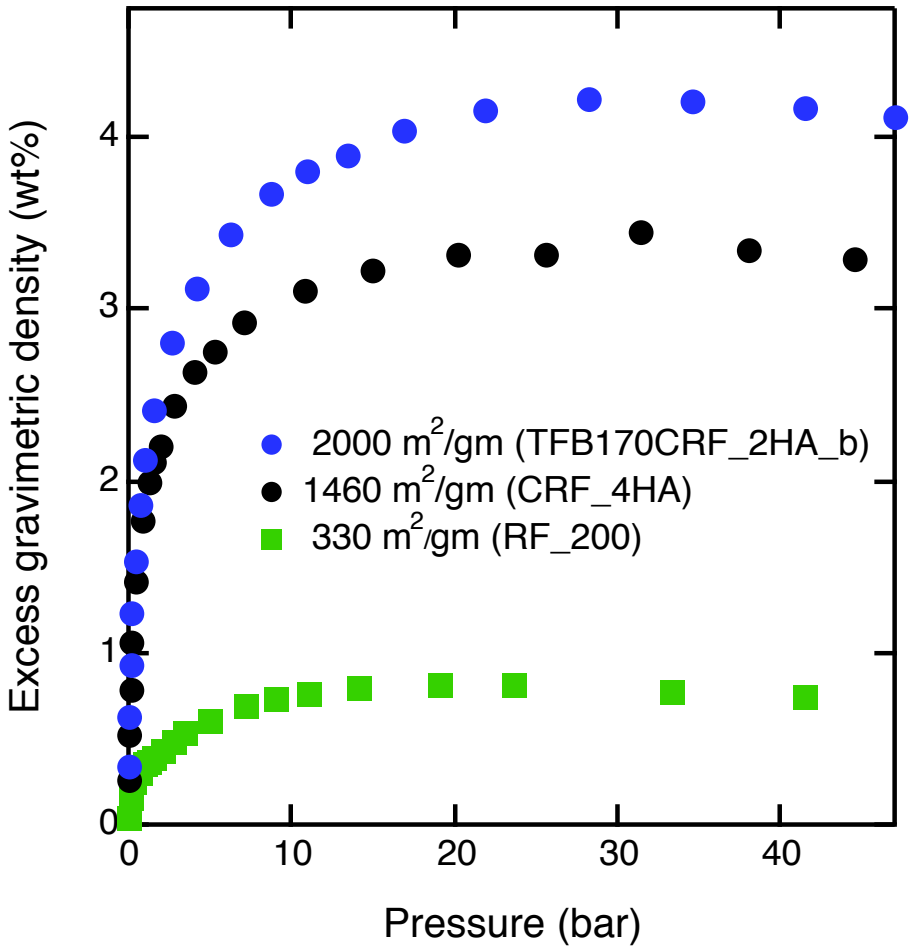

Surface area dependent behavior synthesized by T. Baumann and J. Satcher, LLNL

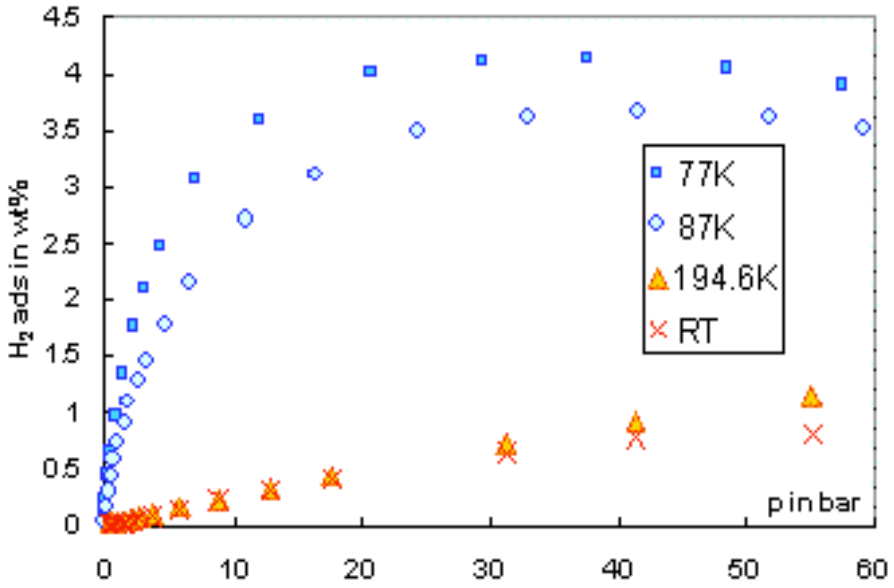

Temperature dependent behavior from IRMOF-1

Why do we get maxima in the adsorption isotherm?

Surface excess adsorption; the gas/solid interface

Volume of adsorbed layer:

$$V^a = Ax_1$$

Amount adsorbed in adsorbed layer:

$$n^a = \int_0^{V^a} c dV = A \int_0^{x_1} c dx$$

Total amount of adsorb-able gas *n* in system:

$$n = A \int_0^{x_1} c dx + c^g V^g$$

$$\boxed{n^a = n - c^g V^g}$$

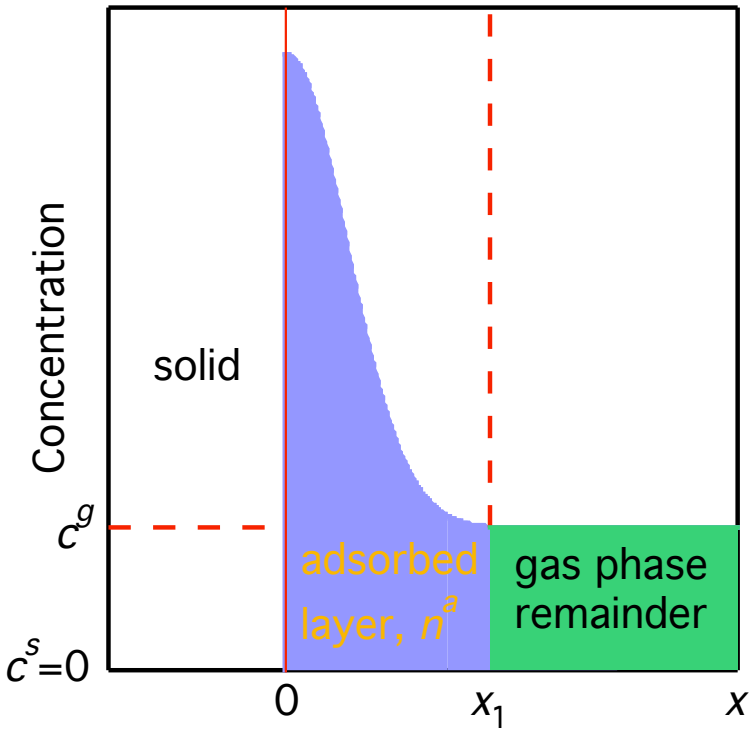

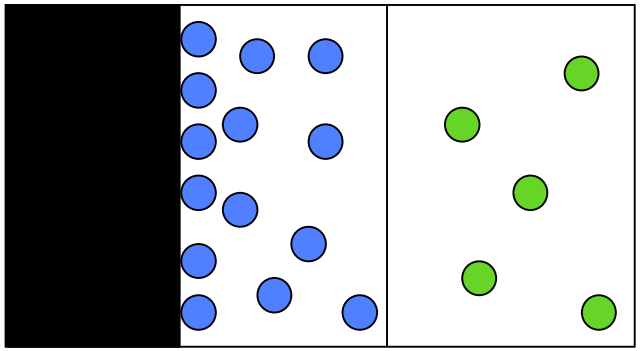

Gibbs dividing plane

For Gibbs dividing surface at solid surface:

$$n^{\sigma} = n - c^{g}V^{g} - c^{g}V^{a}$$

$$\Rightarrow \quad n^{a} = n^{\sigma} + c^{g}V^{a}$$

Assume C^g small and V^a negligible

$$n^{a} \approx n^{\sigma}$$

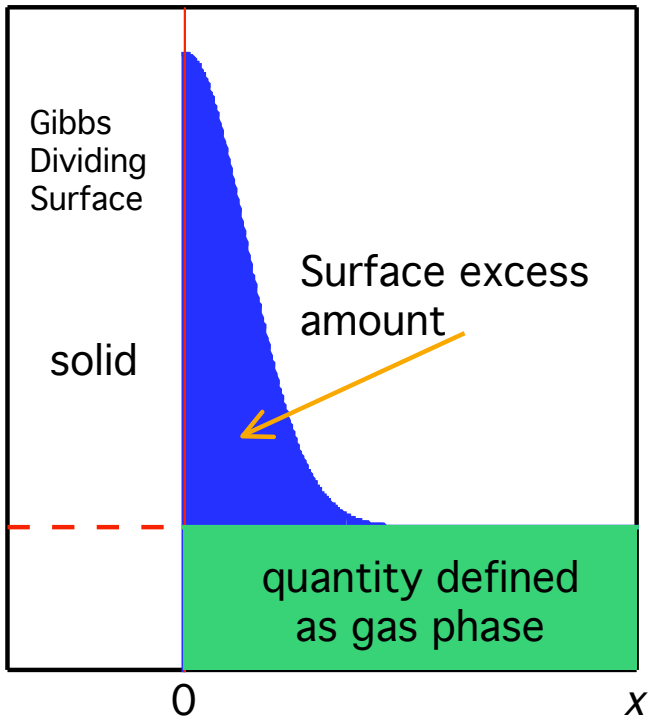

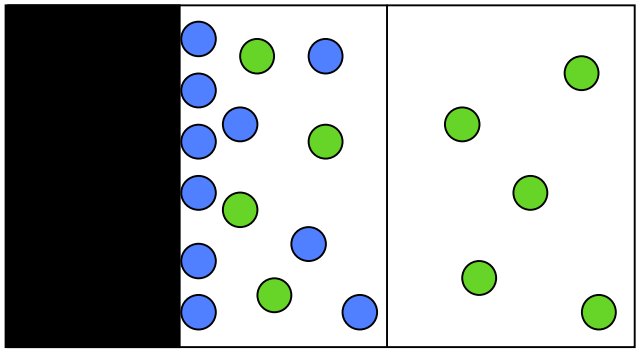

Excess adsorption

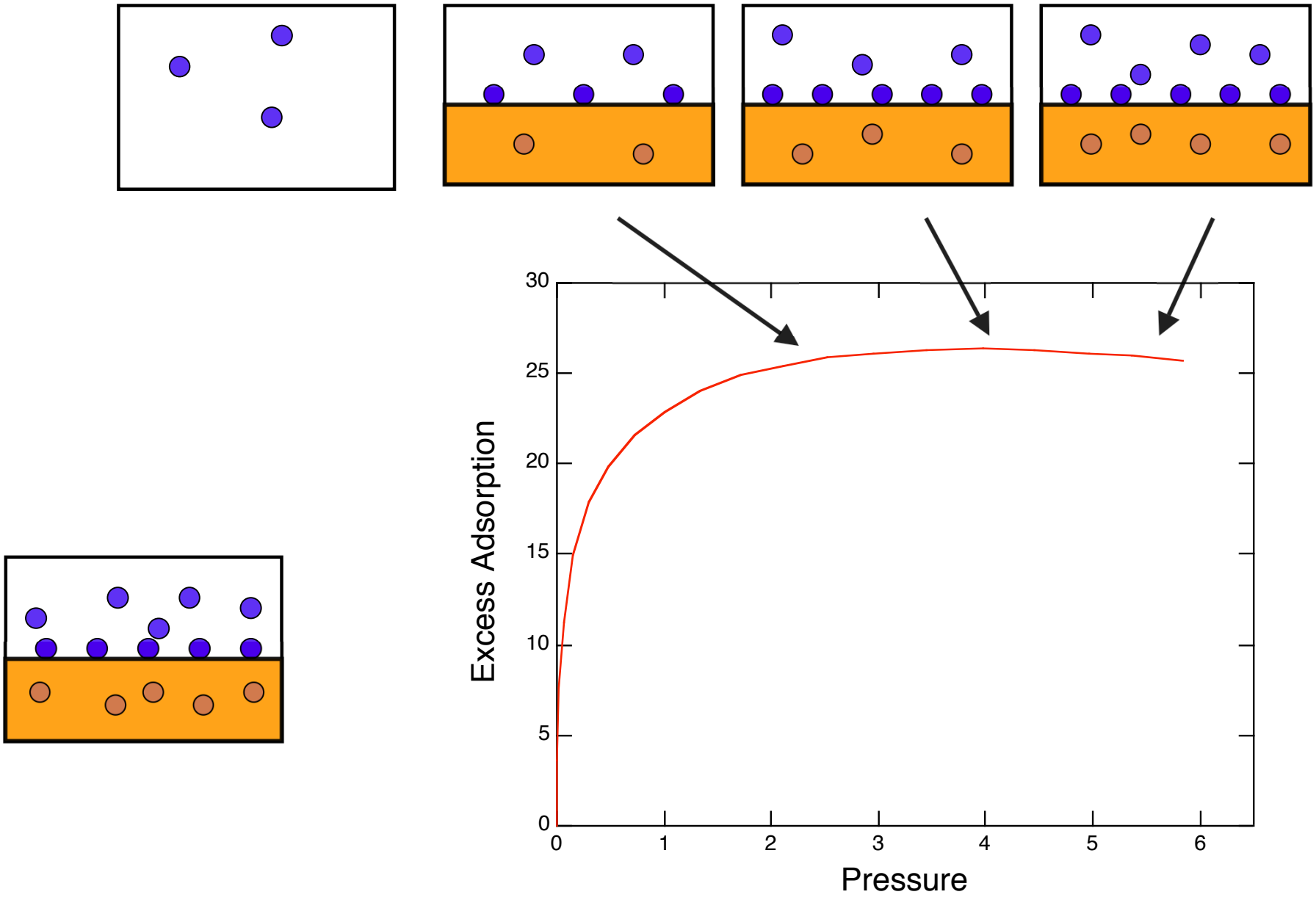

Surface area and micropore/slit pore (< 2 nm) geometry dependencies

Understand gravimetric surface area dependence in aerogels* and other carbons

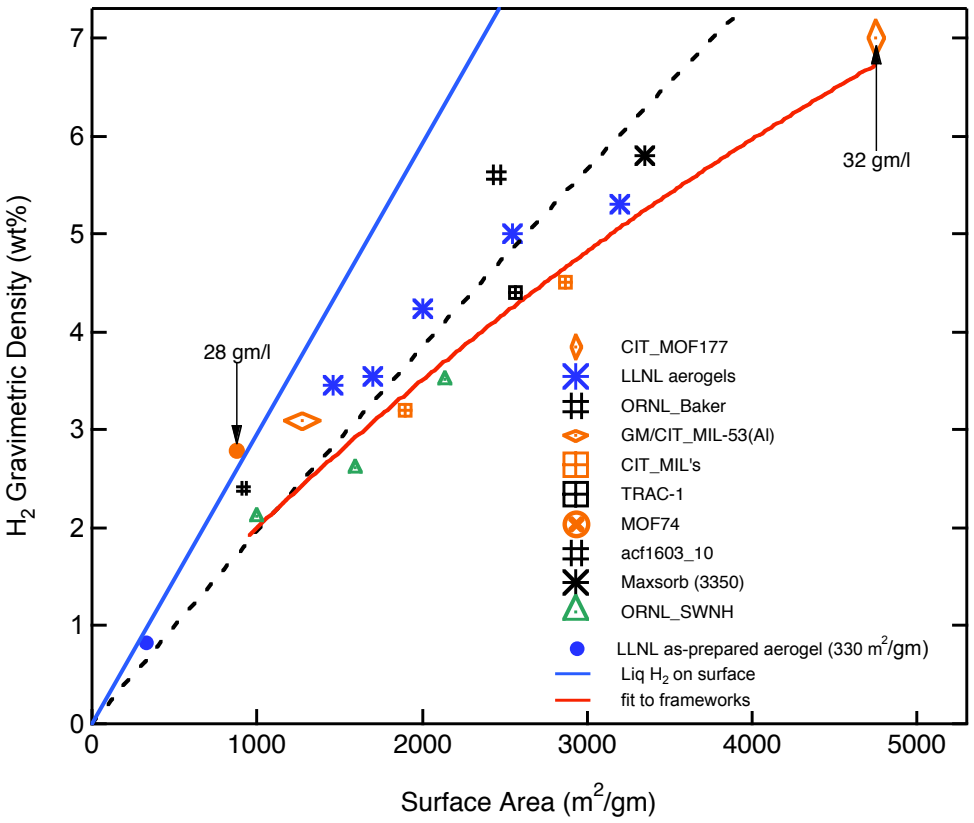

*"Toward New Candidates for Hydrogen Storage: High-Surface-Area Carbon Aerogels," H. Kabbour, T. F. Baumann, J. H. Satcher, Jr., A. Saulnier and C. C. Ahn, Chem Mater, 18, (2006).

Details of micropore/slit pore geometry critical for volumetric optimization

"Characterization and optimization of adsorbents for hydrogen storage," R. Chahine, T. K. Bose, In 11th WHEC, 1996; Pergamon Press: Oxford, U.K., 1996.

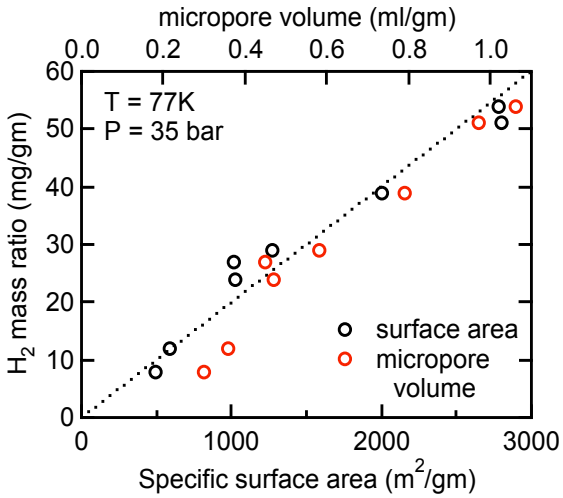

"Molecular simulation of hydrogen adsorption in single-walled carbon nanotubes and idealized carbon slit pores," Q. Wang and J. K. Johnson, J. Chem Phys. 110,(1) (1999).

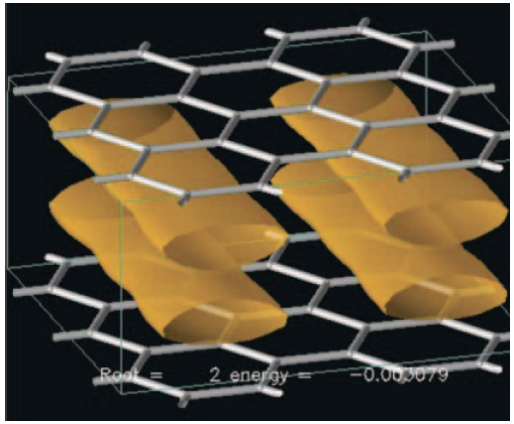

"Graphene nanostructures as tunable storage media for molecular hydrogen" S. Patchkovskii, J. S. Tse, S. N. Yurchenko, L. Zhechkov, T. Heine, and G. Seifert, PNAS, 102(30), 10439, 2005.

How big is molecular hydrogen?

Landolt-Bornstein ($P6_3/mmc$)
solid H_2 at 4.2 K, a=3.76, c=6.14

Koresh and Soffer
liq H_2 (3.62Å, 3.44 x 3.85)

Nielsen, McTague and Ellensen
adsorbed H_2, 3.51Å

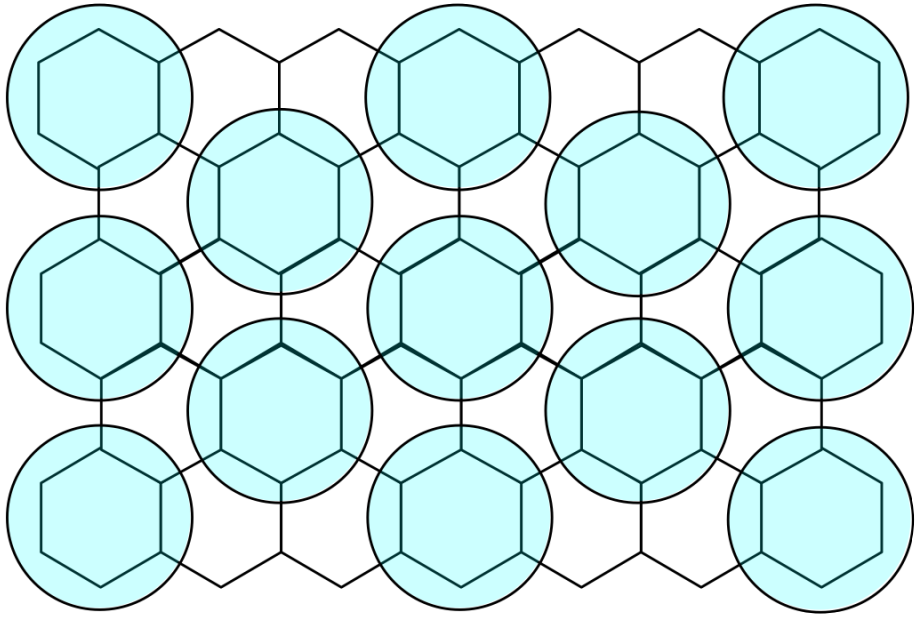

Commensurate $\sqrt{3}$ structure (LiC_6)
or HC_3 => 2.7 wt% (5.4 wt%)

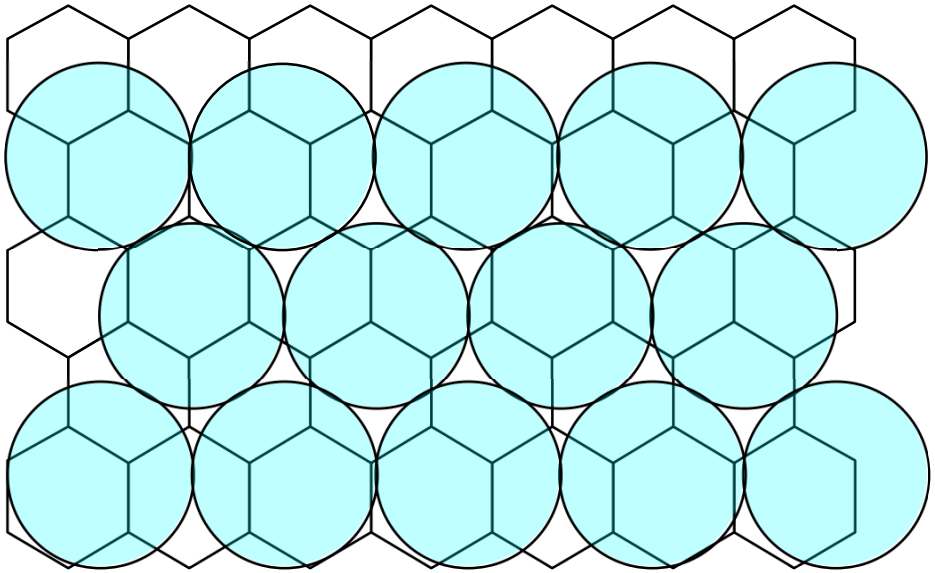

Incommensurate solid H_2 on graphite
=> 3.85 wt% (7.7 wt%).

Range of graphitic structures

Theoretical surface area of a graphene sheet is 2630 m^2/gm.

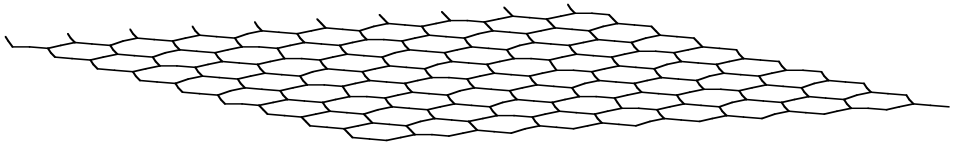

Activated carbons can have higher surface areas of > 3200 m^2/gm, edge components important.

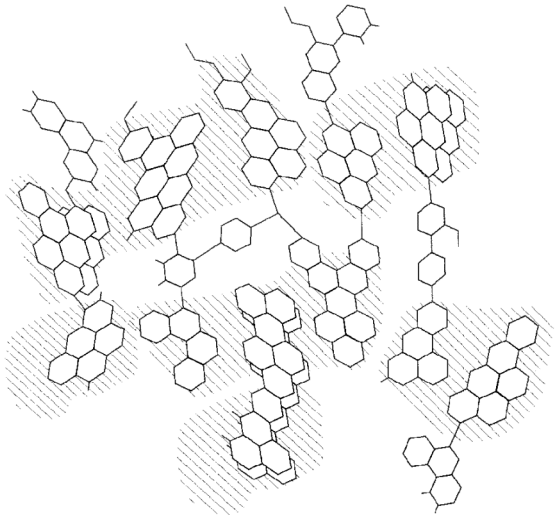

√ 3 structure as x-z cross-section

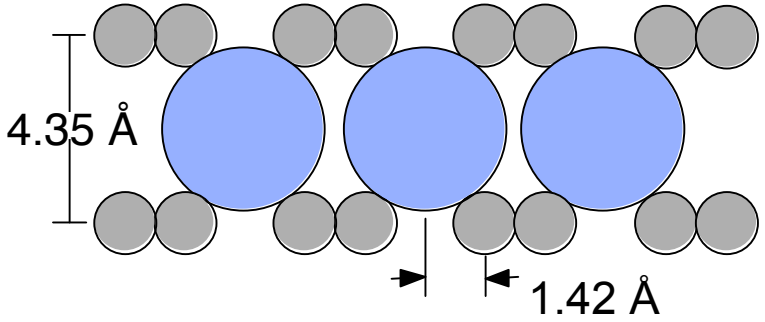

Incommensurate packing as x-z cross-section

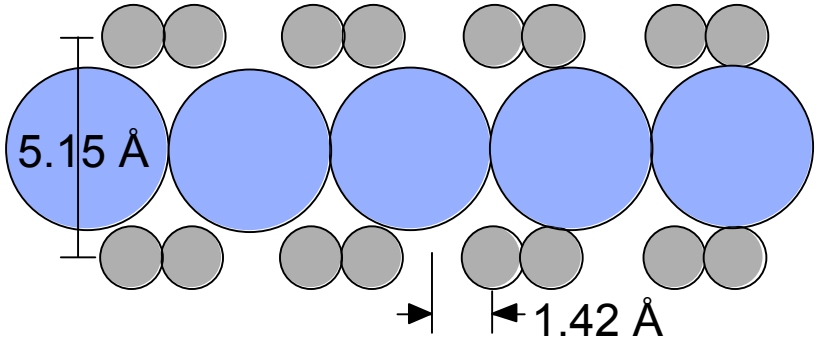

Double packing as x-z cross-section

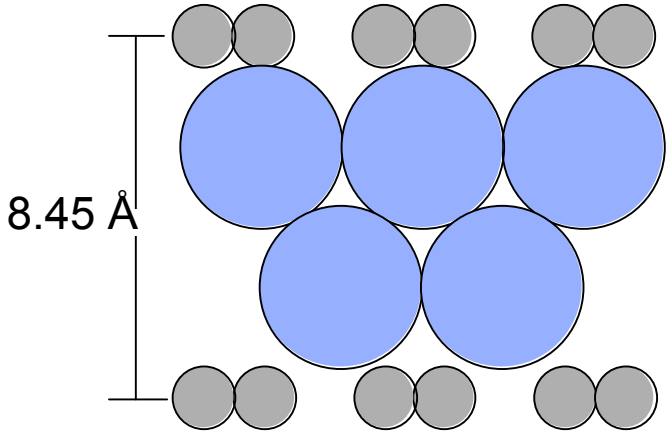

Calculating enthalpies

- Gas adsorption calorimetry

  combines difficulty of calorimetry and gravimetric analysis

- Henry's law (easy to do but applicable at zero coverage pressure):

  $\Pi A = nRT$

  Π spreading pressure

  $n = k_H p$ the specific surface excess amount

  $\ln(n/p) = K_1 + K_2 n + K_3 n^2$

  Advantage is that linearity of semi-log plot extends above Henry's law region.

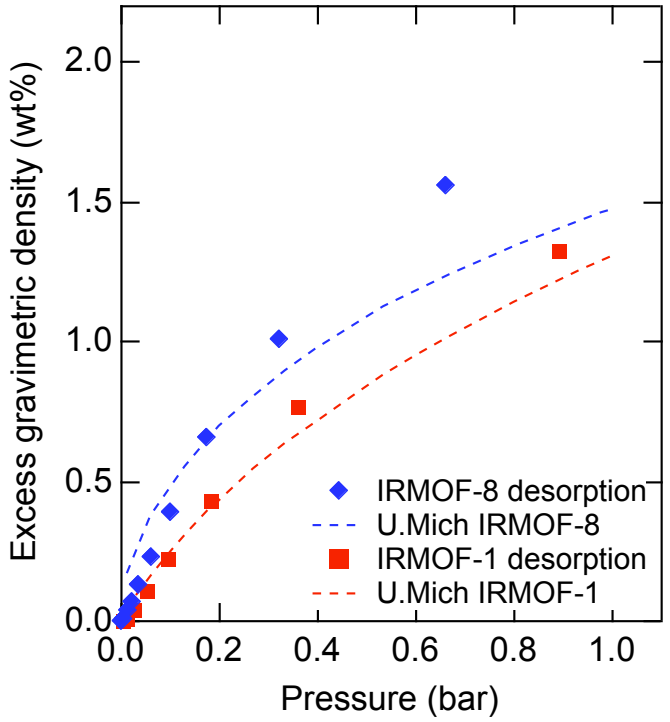

Differential enthalpy of adsorption at 'zero' coverage then

$$\left(\frac{\partial H}{\partial n}\right) = RT^2 \frac{\partial(\ln k_H)}{\partial T}$$

Cole, J. H.; Everett, D. H.; Marshall, C. T.; Paniego, A. R.; Powl, J. C.; Rodriguez Reinoso, F., *J. Chem. Soc., Faraday Trans.* **1974,** I 70, 2154.

Henry's law analysis cont'd

Plot ln(n/p) vs n

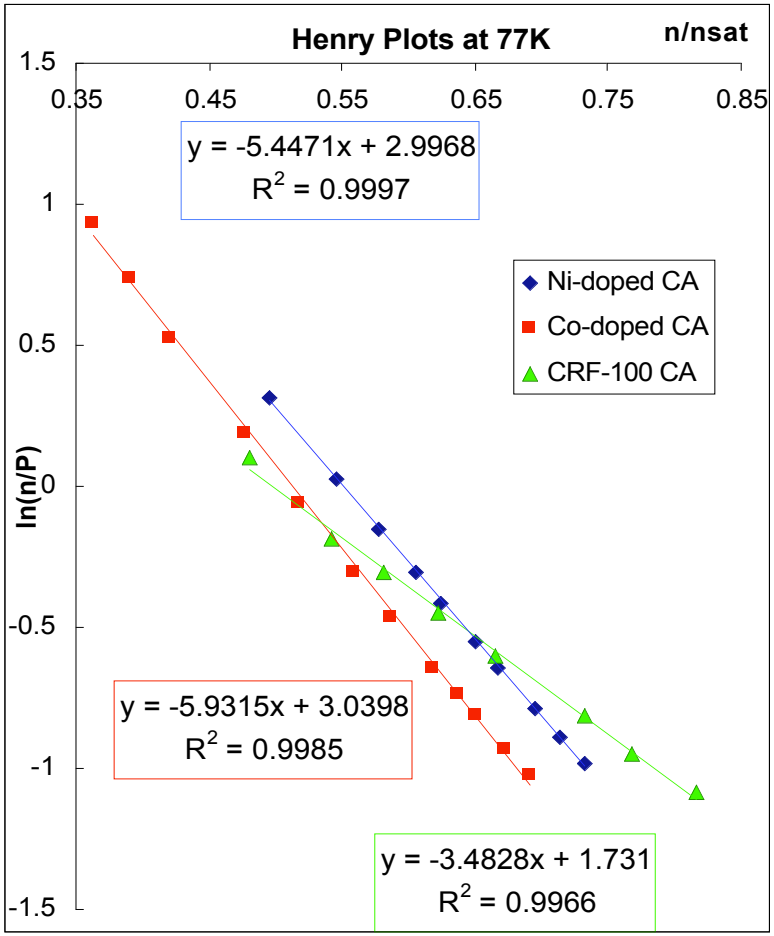

Plot ln(k_H) vs $1/T$

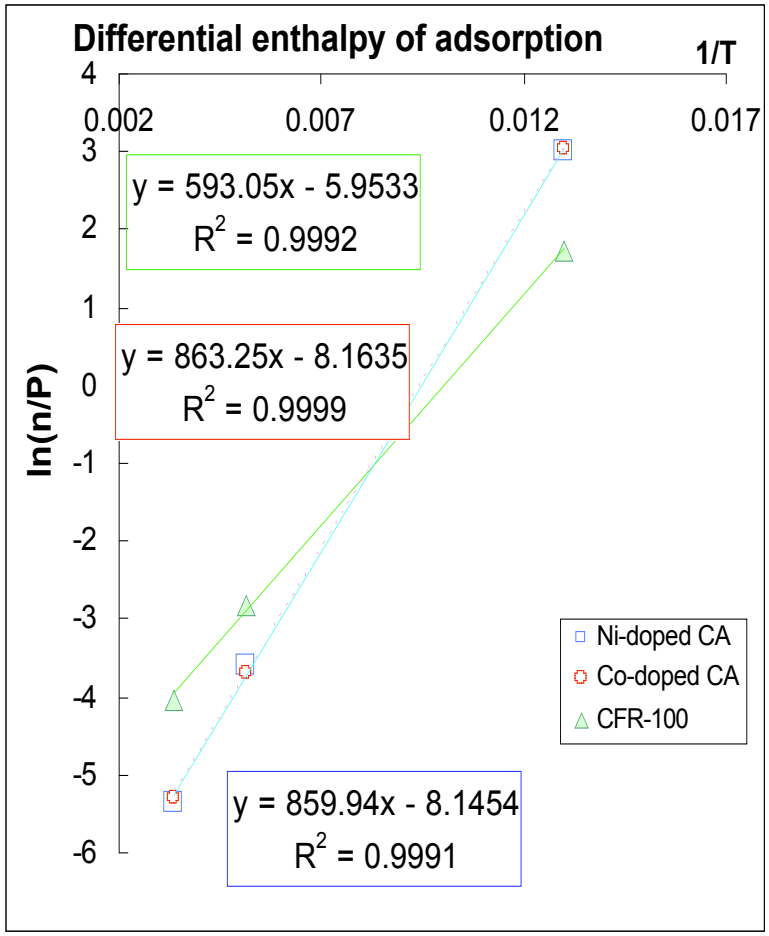

Isosteric enthalpy of adsorption

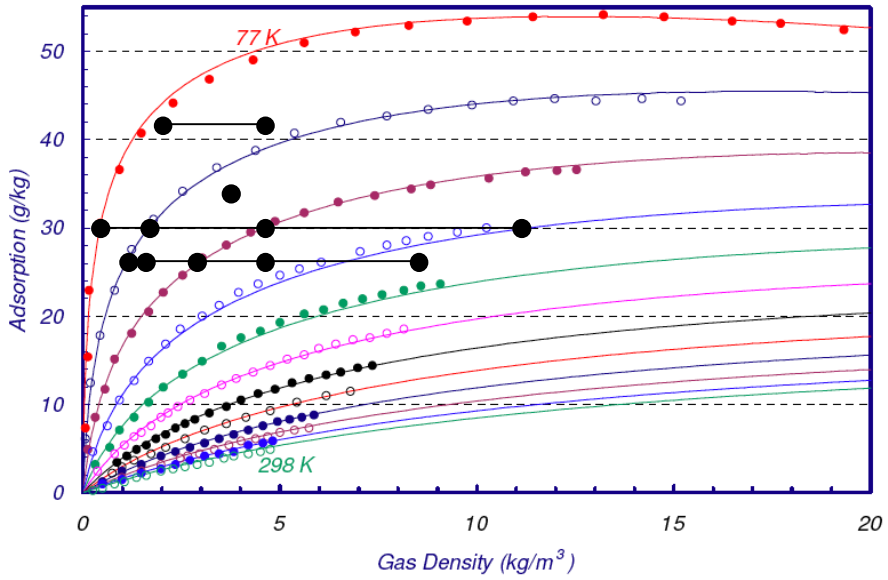

From Benard and Chahine
Int. J. Hydrogen Energy, 26 (2001)

$$\left(\frac{\partial H}{\partial n}\right) = R\left(\frac{\partial \ln p}{\partial 1/T}\right) = -\frac{RT_1T_2}{T_2 - T_1}\ln\frac{p_2}{p_1}$$

Data from IRMOF-1

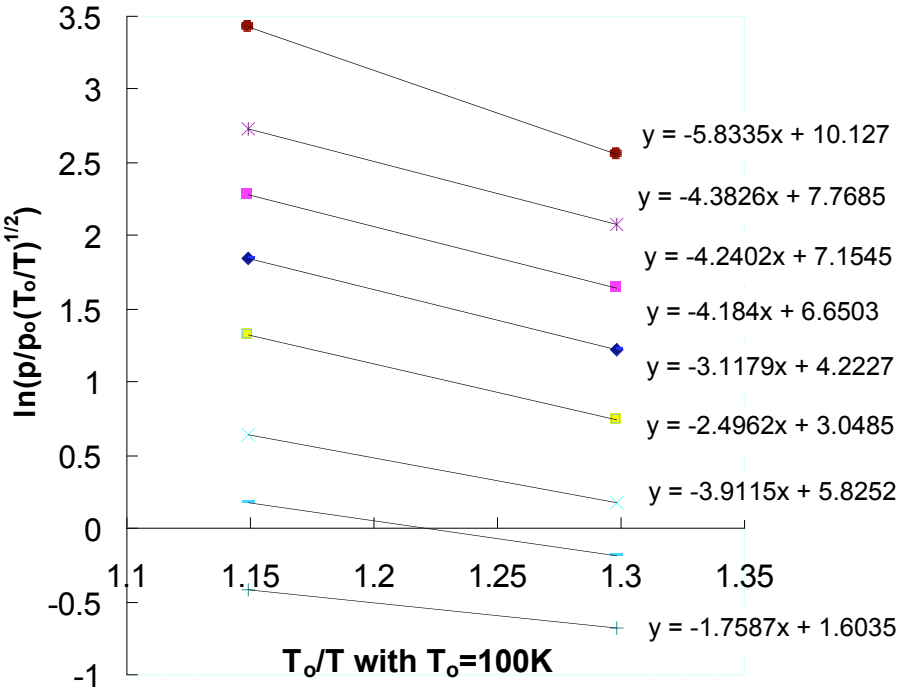

Rouquerol, F.; Rouquerol, J.; Sing, K., *Adsorption by Powders and Porous Solids*. Academic Press: New York, 1999.

Increasing molecular hydrogen density via a micro-porous framework structure, MOF-74

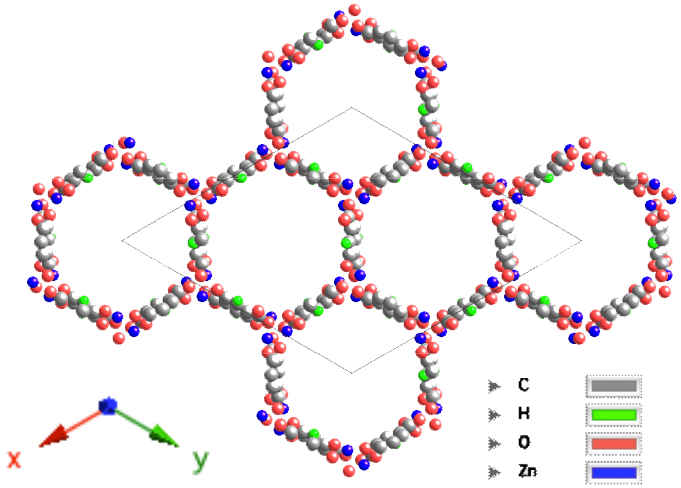

MOF-74 as shown above, one of the few examples of a microporous metal organic framework. R-3 space group a=25.9 Å and c=6.8 Å. Zinc octahedra (ZnO_6) share edges and form long chains parallel to c-axis. Organic units link chains leading to channeled structure with small hexagonal windows of ~ 11Å diameter. Chains provide high density of exposed metallic sites. Bulk density of 1.2 gm/cc. Synthesis of 2 gms required 2 months.

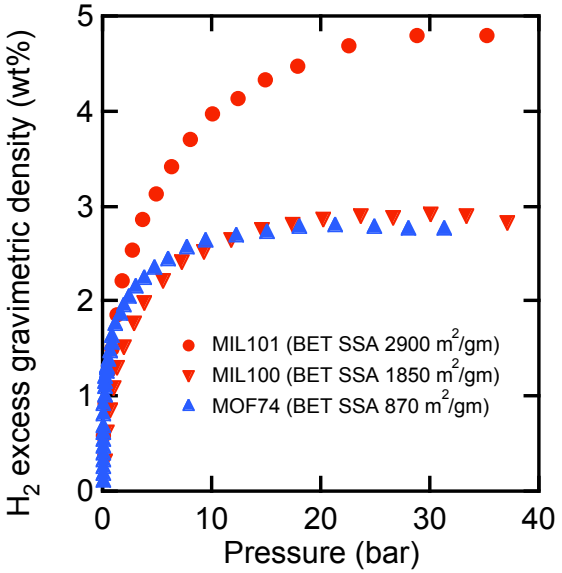

Isotherm at left shows that MOF 74 with SSA of 870 m^2/gm has surface excess sorption comparable to a typical 1850 m^2/gm sorbent (here compared with MIL100 and MIL101). Attributed to high surface density of molecular hydrogen. Volumetric density of 33 kg/m^3.

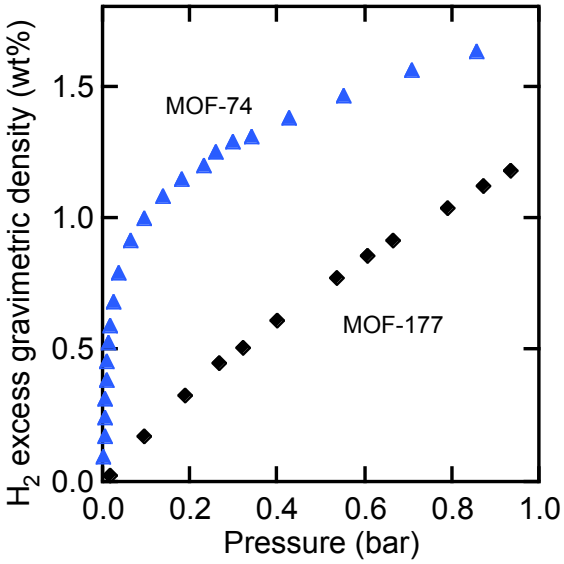

Sharper initial isotherm seen at left indicates higher sorption enthalpy in Henry's law region.

Closest hydrogen near neighbor distances in MOF 74 as determined at NIST

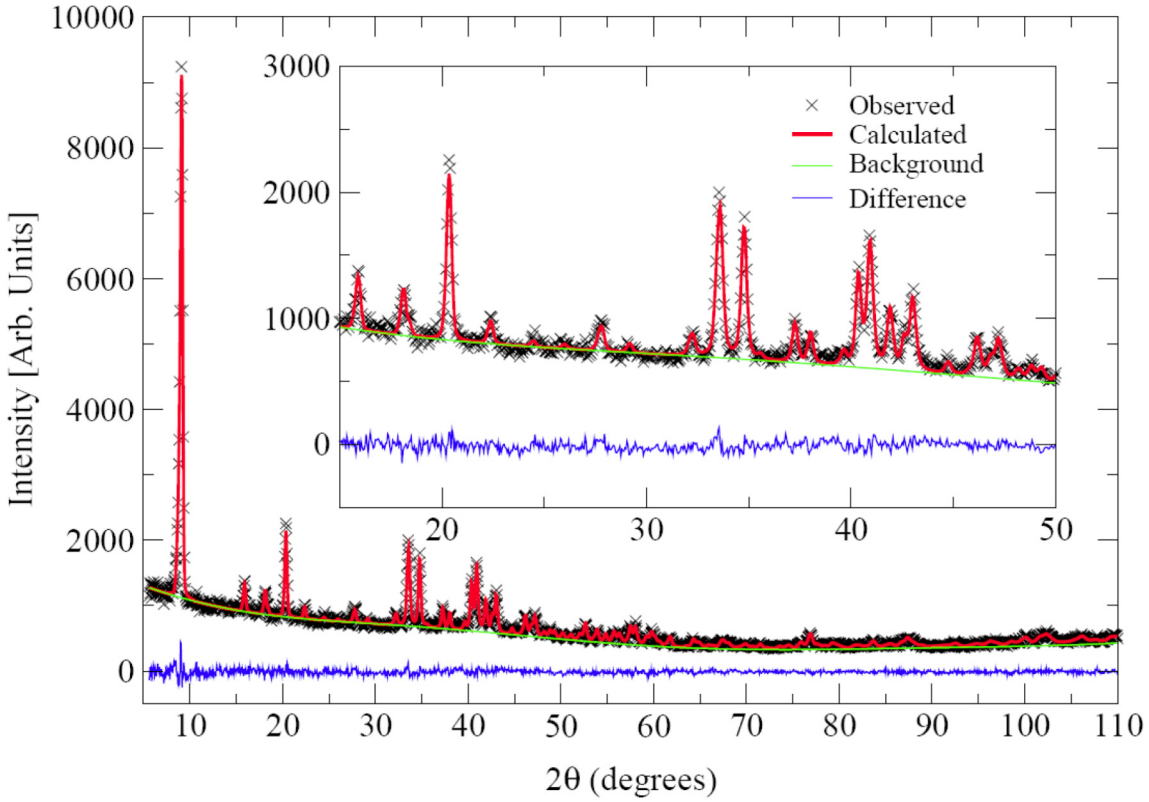

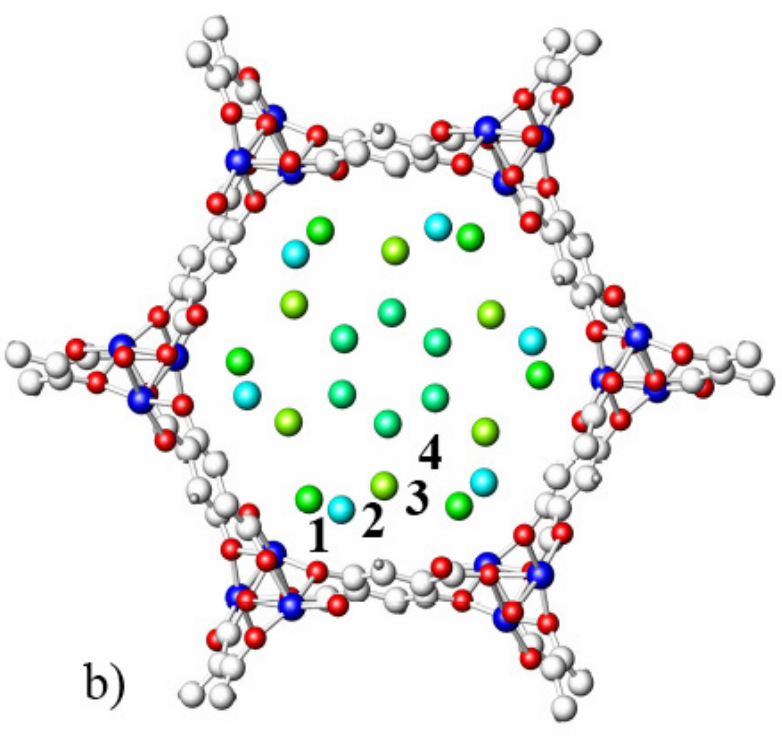

Rietveld refinement and neutron powder diffraction data for a loading at 3.0 D_2:Zn (model showing loading positions at right). Cross, red line, green line, and blue line represent the experimental diffraction pattern, calculated pattern, calculated background, and the difference between experiment and calculated patterns. Data were collected using 2.0787 Å wavelength neutrons.

"Increasing the density of adsorbed hydrogen with coordinatively unsaturated metal centers in metal-organic frameworks," Yun Liu, Houria Kabbour, Craig M. Brown, Dan A. Neumann, Channing C. Ahn, Langmuir published online March 27, 2008, 10.1021/la703864a

Henry's law heat for MOF-74

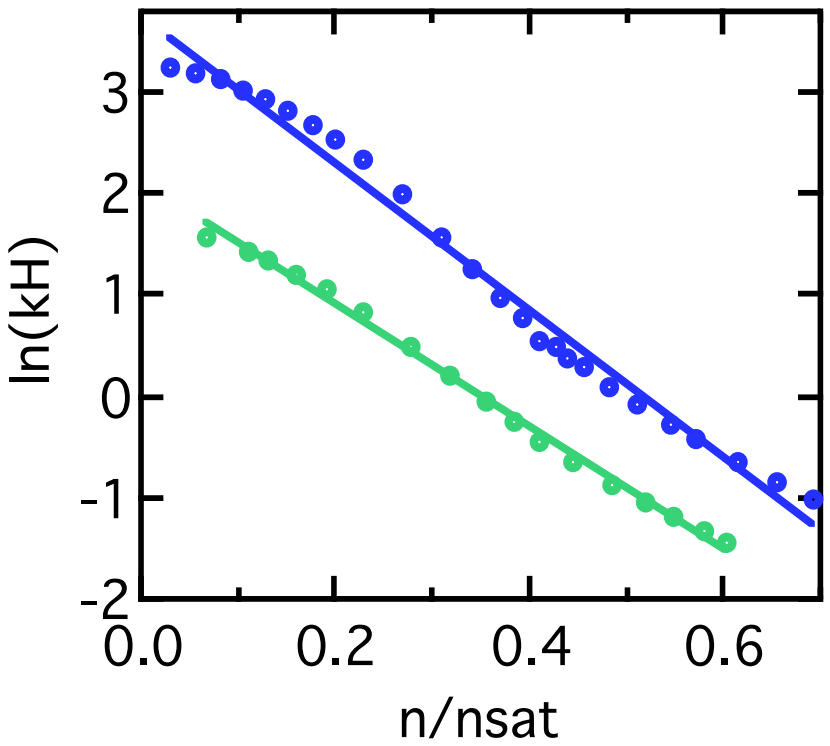

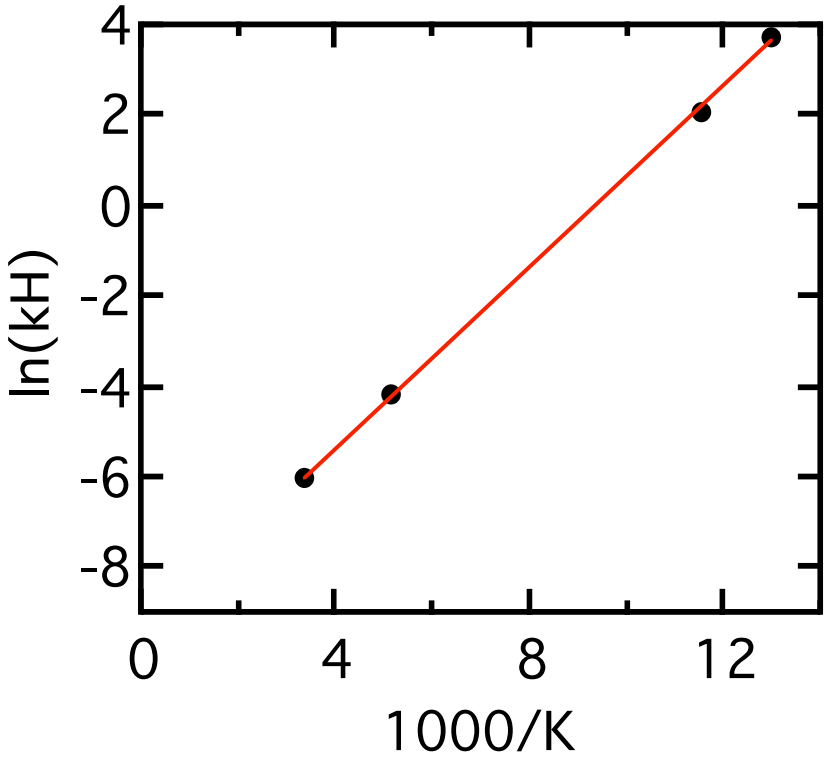

Henry's law region (differential enthalpy of adsorption at zero coverage) the heat of initial H_2 molecule adsorbed onto surface. Non-linearity of semi-log fit an indication of heterogeneity in sorption site.

Seen at both 77 and 87K.

Henry's law fit indicates -9.4 kJ/mole differential enthalpy of adsorption at zero coverage.

$$\left(\frac{\partial H}{\partial n}\right) = RT^2 \frac{\partial(\ln k_H)}{\partial T}$$

H_2 site occupancy and isosteric heat in MOF 74

- Isosteric enthalpy of adsorption tracks enthalpy vs coverage. Initially loaded site above coordinatively unsaturated Zn as determined by neutron diffraction (NIST).
- Near neighbor 2.85 Å D_2-D_2 spacing (site 1 to site 3) helps explain high surface packing density (range from 2.85 to 4.2 Å). 2.85 Å the closest packing of D_2 seen under these conditions! Normally 3.4 Å on graphitic carbon (~3.6 Å in liq H_2).
- Isosteric enthalpy of adsorption shows drop by nearly a factor of 2 as a function of loading. Site heterogeneity an issue.

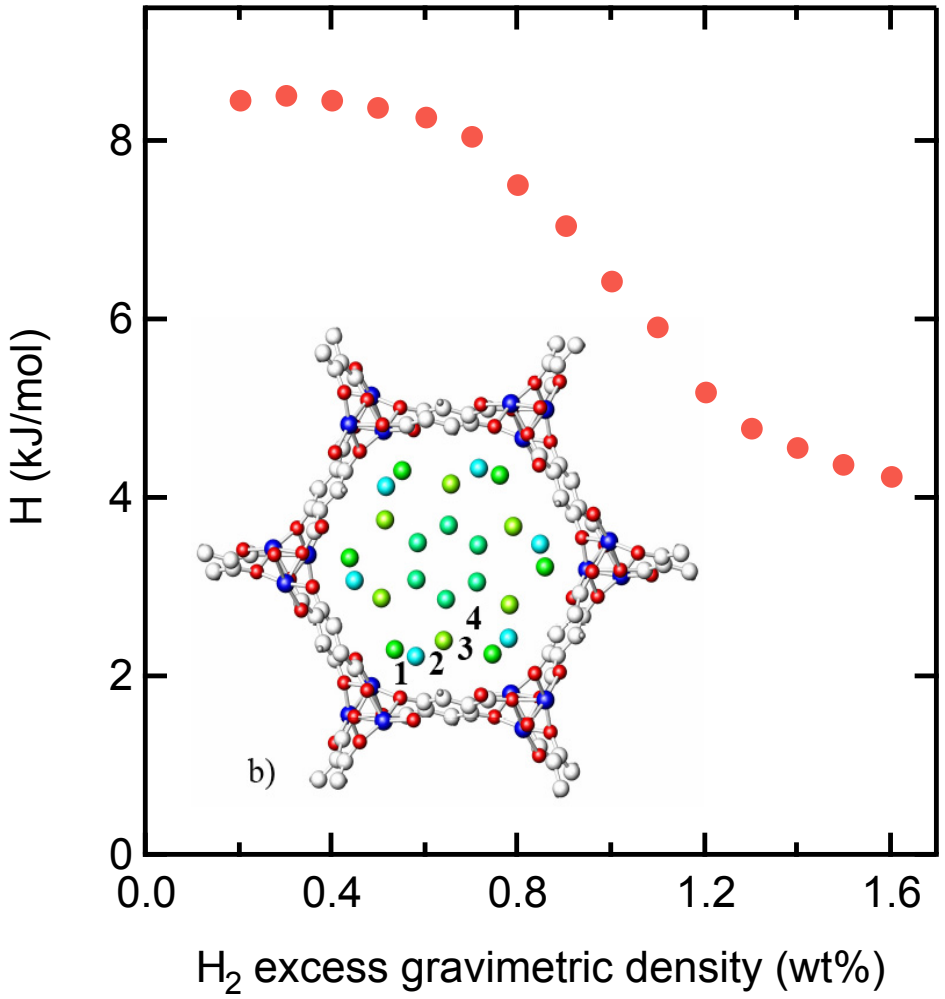

Concept tank based on cryo adsorption

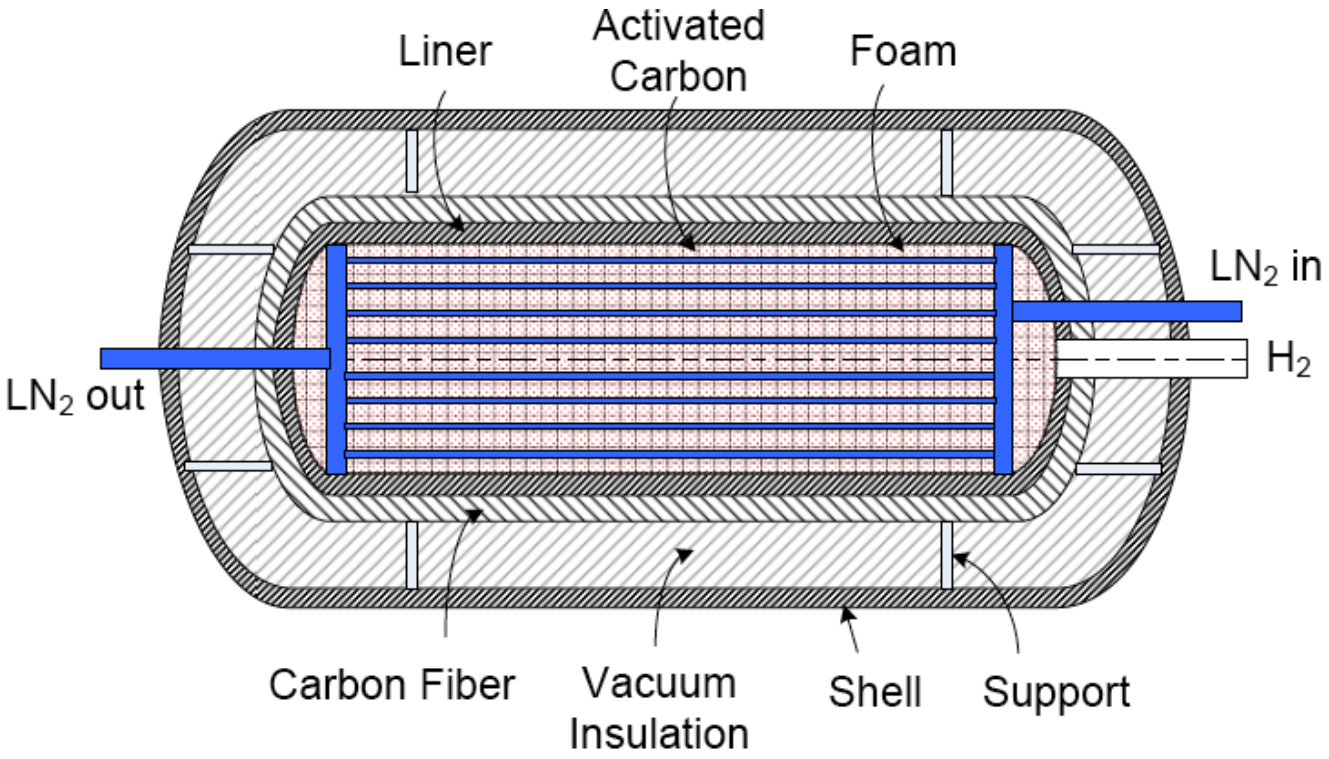

R. Ahluwalia
Argonne Natl Lab

Assume 4kJ/mole sorption heat, and 0.5kg/min refueling rate, then total power dissipation needs to be, for 5 kg of H_2 is ~16kW, considering only sorption heat

Volumetric activated carbon (AC) analysis

Say high surface area AC ~0.3 gm/cc packing density and
Given 2.1 gm/cc skeletal density, let's start with 1 liter volume

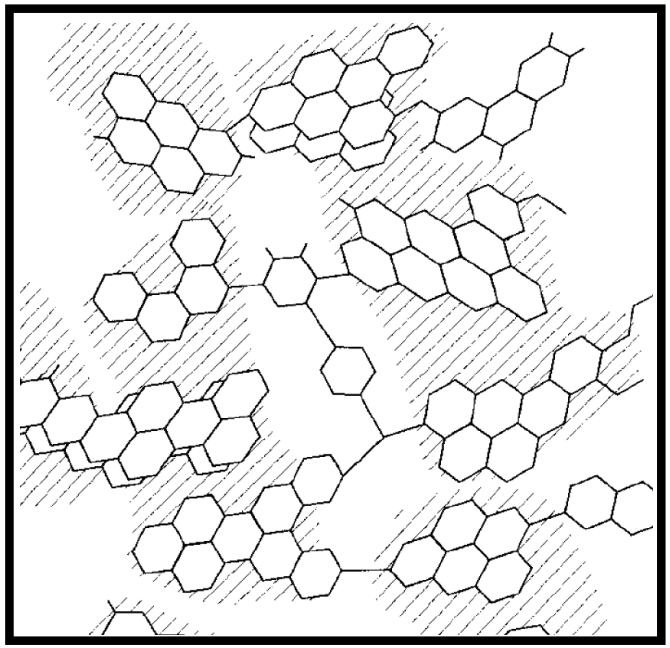

At 0.3 gm/cc 1 liter => 300 gm of AC and 300gm/2.1gm/cc or ~0.143 liter volume occupied by graphitic carbon.

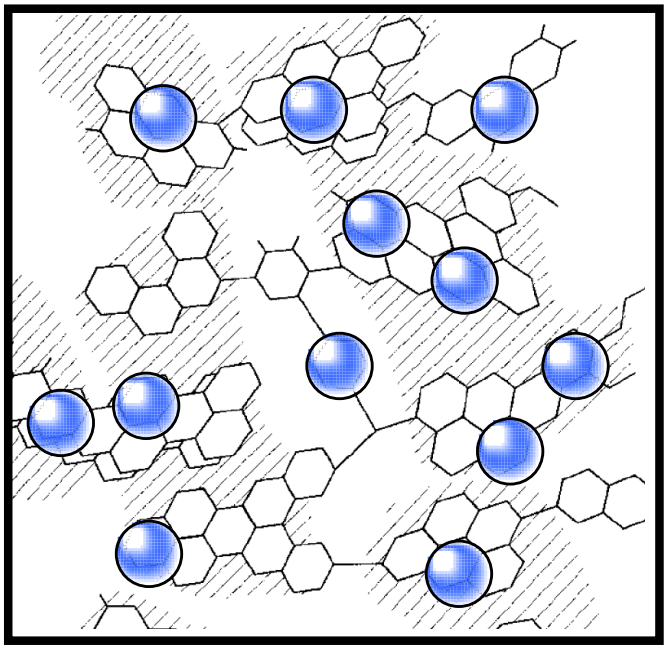

For a 5.5wt% hydrogen storage value, ~17.5gm H_2 in 1 liter. If density of adsorbed layer similar to LH_2 density, then ~250 cc is occupied by adsorbed H_2 gas and ~600cc is left as "free" volume.

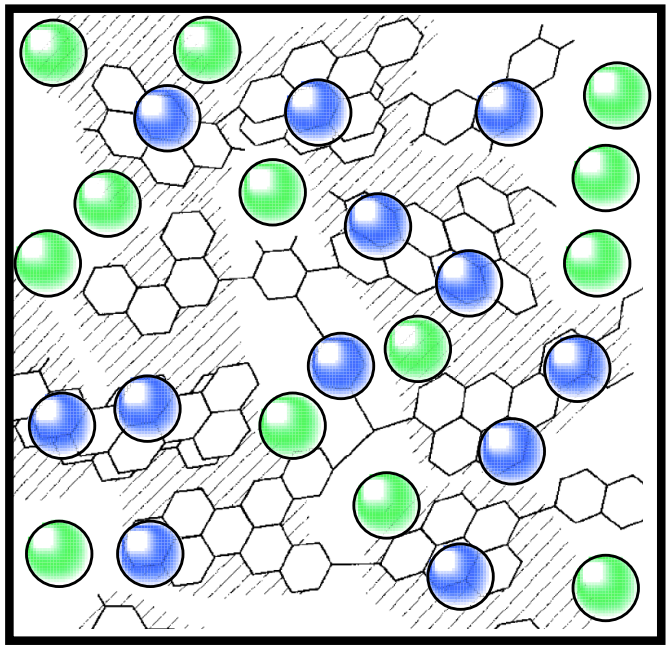

Let's fill remainder of void (~600cc) with H_2 using gas law.

Gas law contribution to remaining void

For an activated carbon then, where:

R=83.14 cc bar/mol K

At 77K, for pv/RT=n,

$$\frac{40 \text{ bar} * 600\text{cc}}{(83.14 \text{ cc bar/mol K}) * 77\text{K}}$$

= 3.75 mol or 7.5 gm H_2

Add this to 17.5 gms H_2 adsorbed so get ~25 gm/liter total

Our "1 liter tank" has a total adsorbed and gas volume density of 25g H_2/300gm AC/liter or 7.8wt%

A tank with 5kg capacity should then have an interior volume of ~200 liters.

Let's apply this analysis to IRMOF-1

Total density is 0.6gm/cc and skeletal density is 2.9gm/cc.

In 1 liter, 600gm/2.9gm/cc -> 0.2 liters of skeletal density of IRMOF.

Be generous and assume 5wt% => 32 gms hydrogen stored and assume this 32 gms occupies ~0.46 liters of "adsorbed" space.

Add this 0.46 liters of 'adsorbed' H_2 to 0.2 liters of IRMOF skeletal density and have 0.34 liters "free" volume to apply gas law to get an additional 2.1 gms H_2 so ~34 gms total in 1 liter (~5.3wt%) or

147 liter interior volume for 5 kg storage.

Let's optimize the carbon structure

Want graphitic structure with 2 out of 3 planes removed.

Now we have instead of 2.1gm/cc as in graphite, ~0.7 gm/cc packing density use all interlayer space to pack H_2 at 7.7wt%.

Given 2.1 gm/cc skeletal density, let's start with 1 liter volume

1 liter will have 700 gm of this idealized carbon, assume at 7.7wt%, this carbon will hold ~58 gms/liter

=> <u>86 liter tank</u> necessary to store 5 kg of H_2.

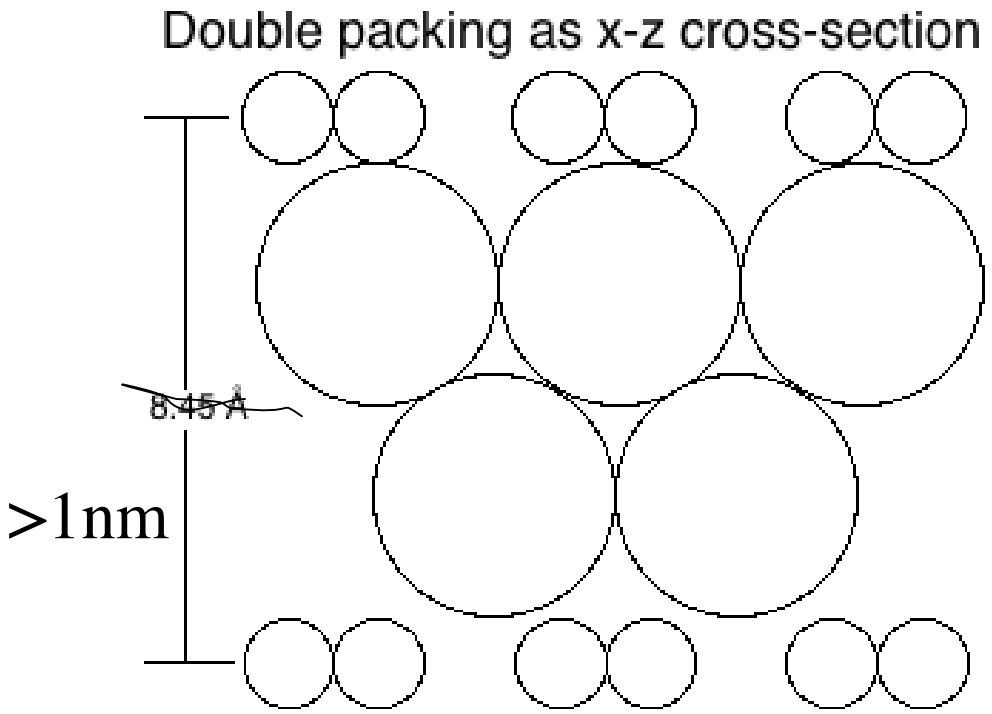

Summary of physiorption in aerogels and coordination polymers

- Differential enthalpy of adsorption at ‘zero’ coverage different than isosteric enthalpy of adsorption (which generally decreases with hydrogen loading).
- Higher surface aerogels behave as most carbons adsorbing ~1wt%/500m^2/gm so goal should be to produce as high a surface area sorbent as possible.
- Pore size should be optimized to be ~1 to 1.1nm to maximize volumetric density.
- Coordination polymers interesting but overall gravimetric/volumetric density properties not much better than carbons.

Equilibrium Behavior of Metal Hydrides

Dissociation pressure isotherms for Li-LiH[1]

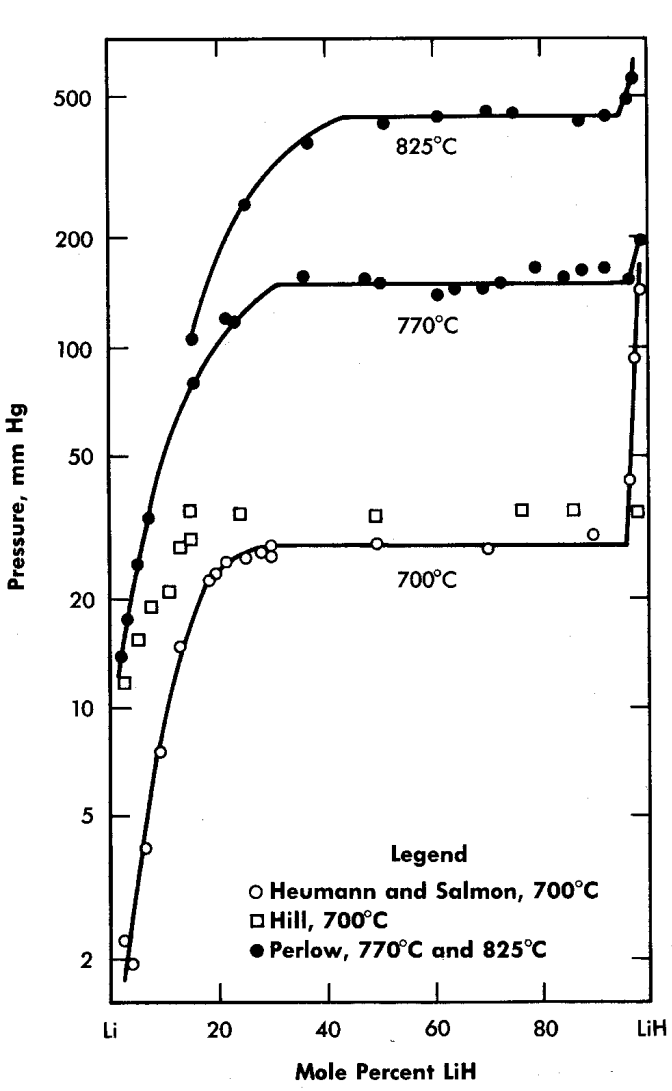

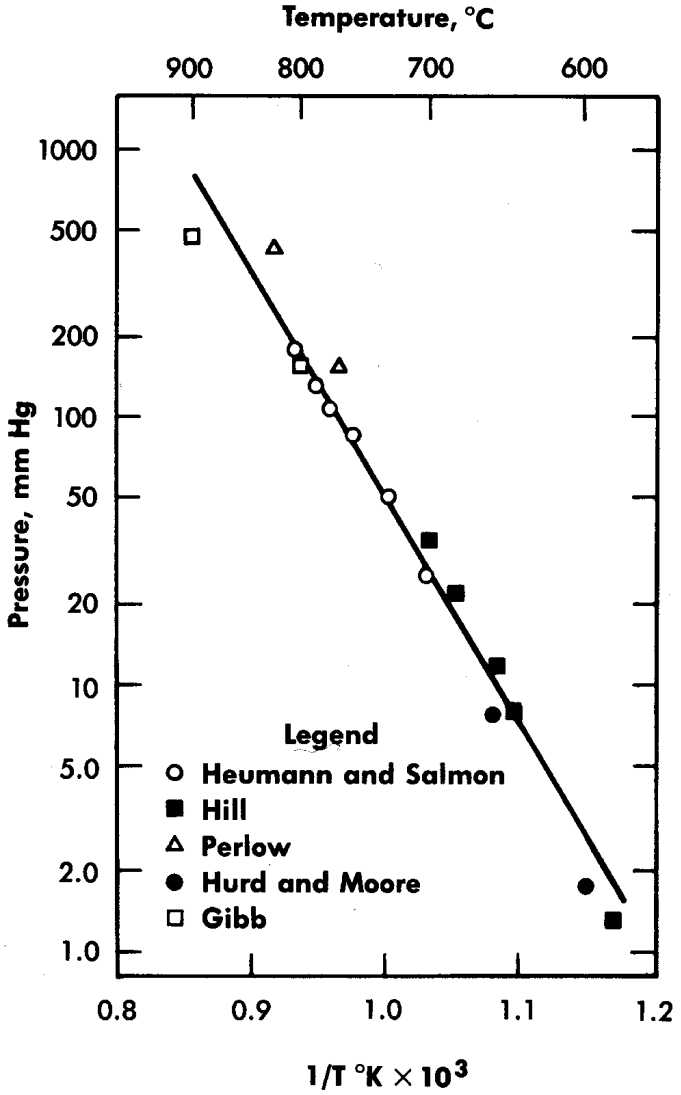

Equilibrium pressure vs condensed phase comp.

Plateau pressure region where pressure independent of composition.

3 phases in equilibrium, two condensed phases and H_2 gas.

Assumptions:

1) phase on left a saturated solution of hydride in metal.

2) phase on right saturated solution of metal in hydride.

3) chemical reaction of plateau region is:

$$\frac{n}{2}\mathrm{H_2(gas)} + \mathrm{M(s)} \rightleftharpoons \mathrm{MH}_n\mathrm{(s)}$$

[1]C. E. Messer, “A survey report on lithium hydride,” USAEC Report NYO-9470, 1960

van't Hoff data for the Ca-CaH_2 system

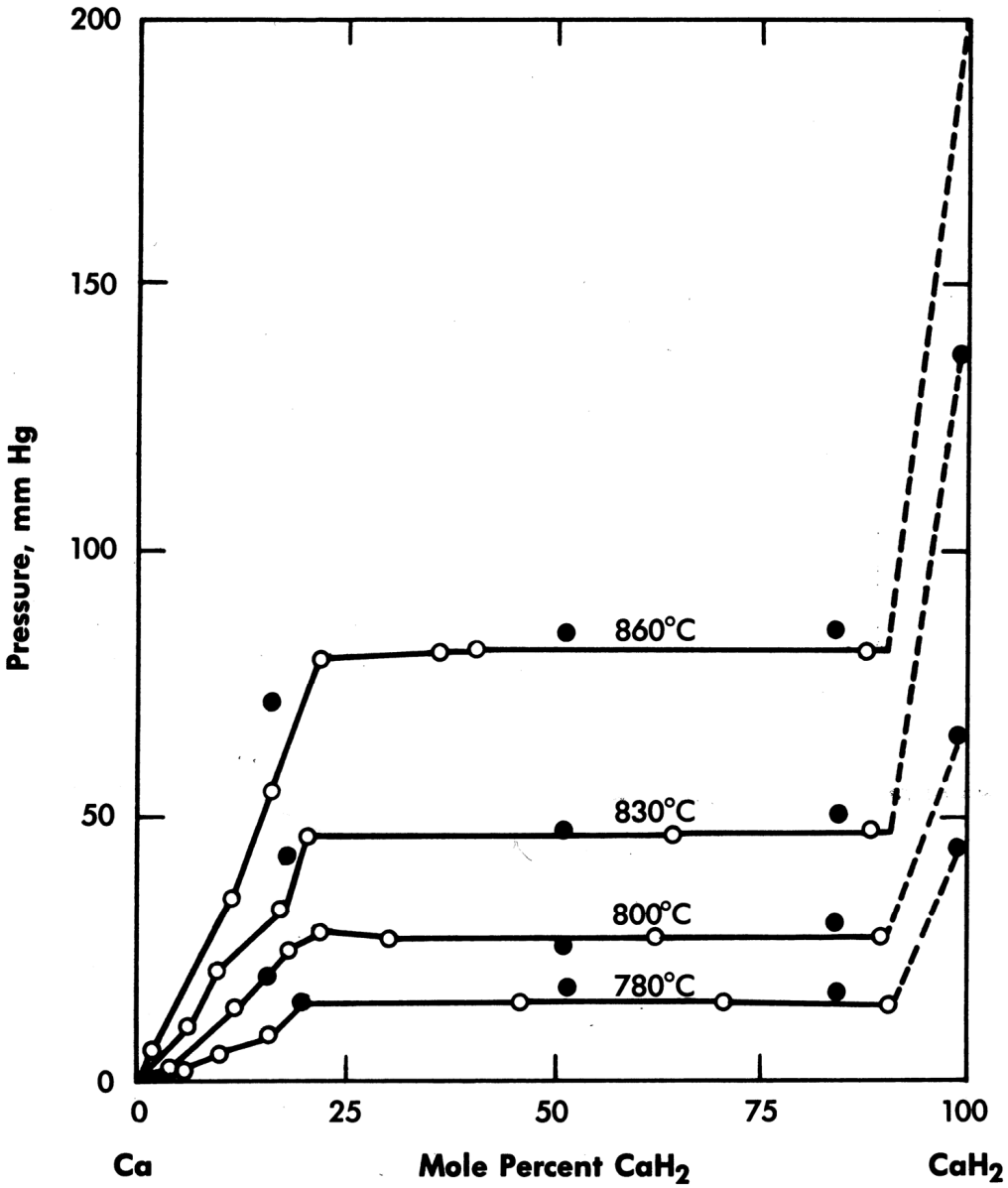

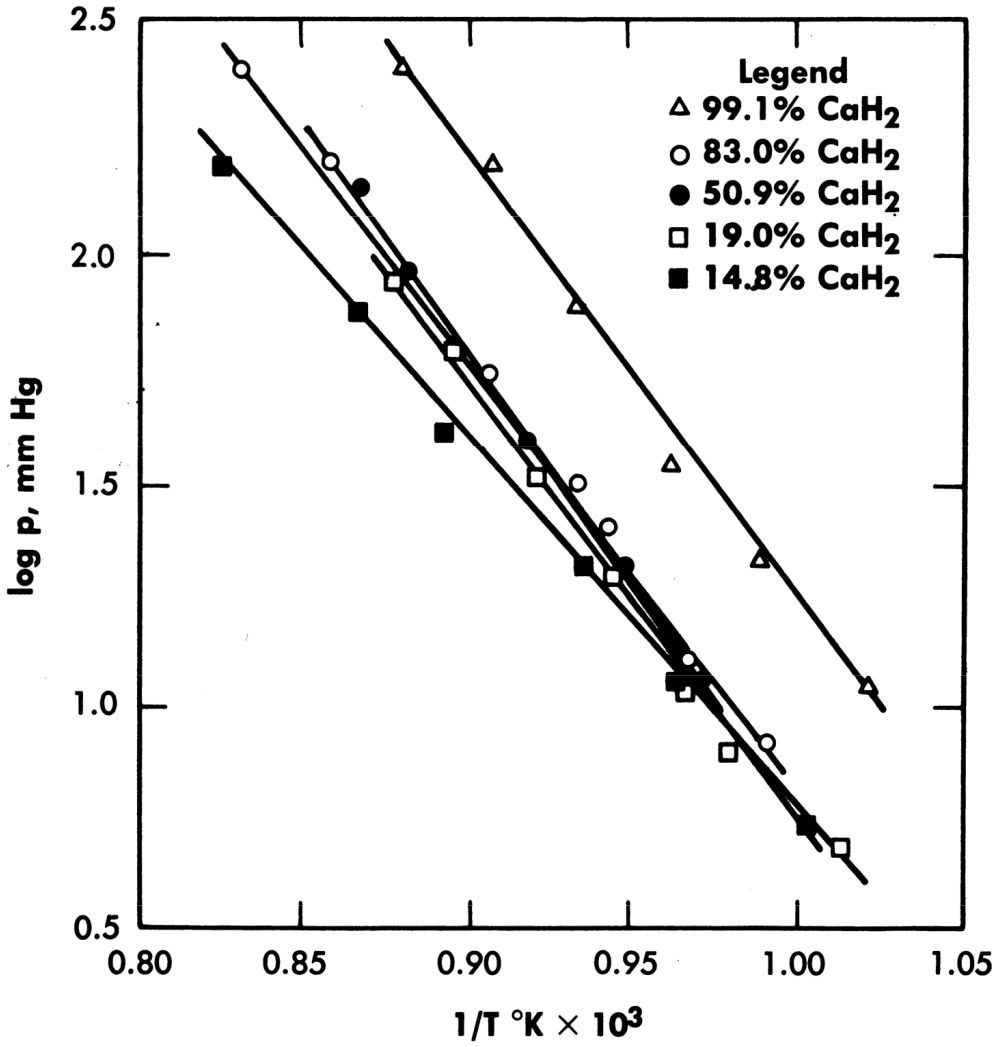

From W.D. Treadwell and J. Sticher, "Uber den Wasser-stoffdruck von Calciumhydrid, Helv. Chim. Acta 36 (1953)

Equilibrium Behavior of Metal Hydrides

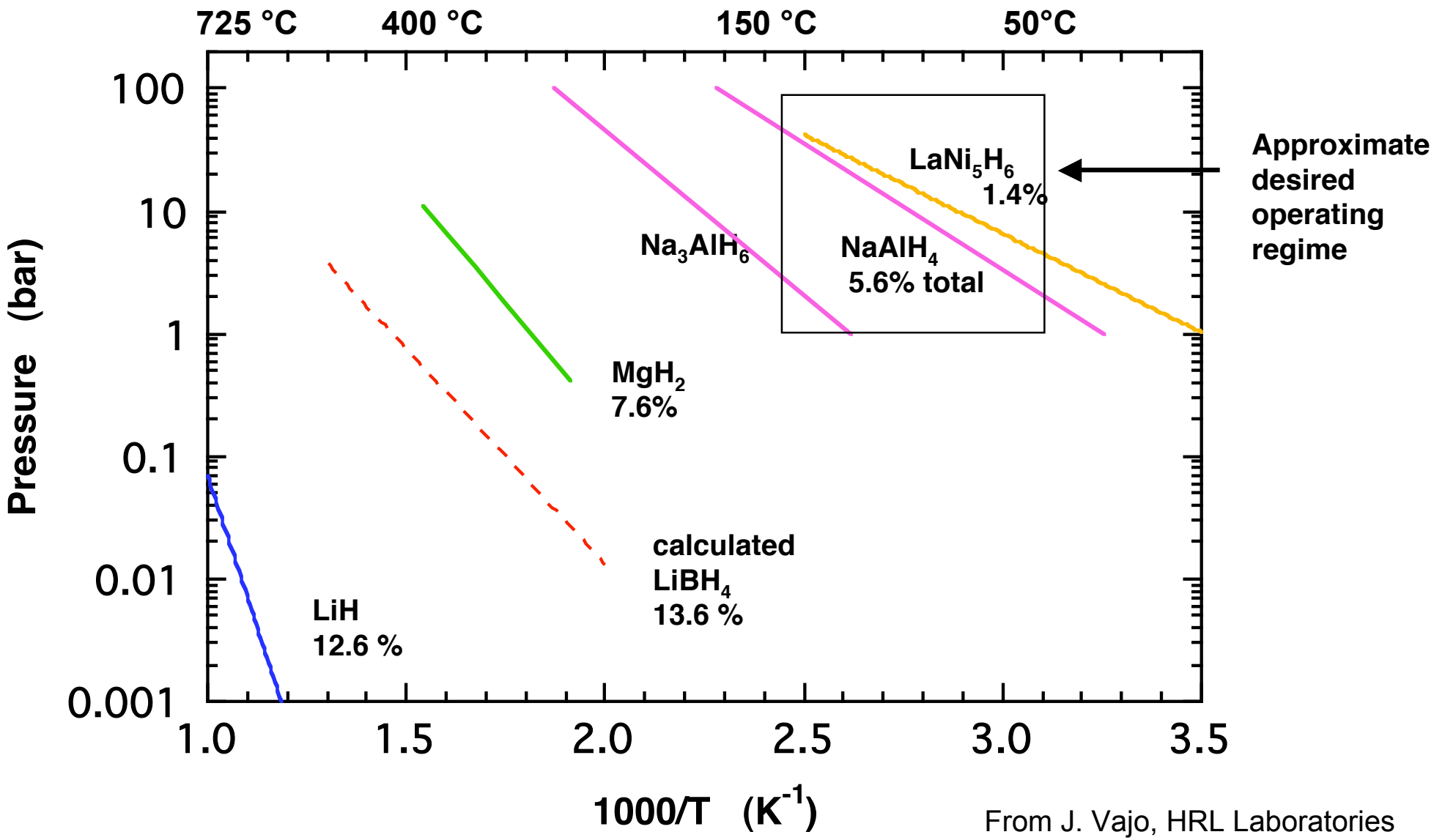

From J. Vajo, HRL Laboratories

Destabilizing high ΔH hydrides

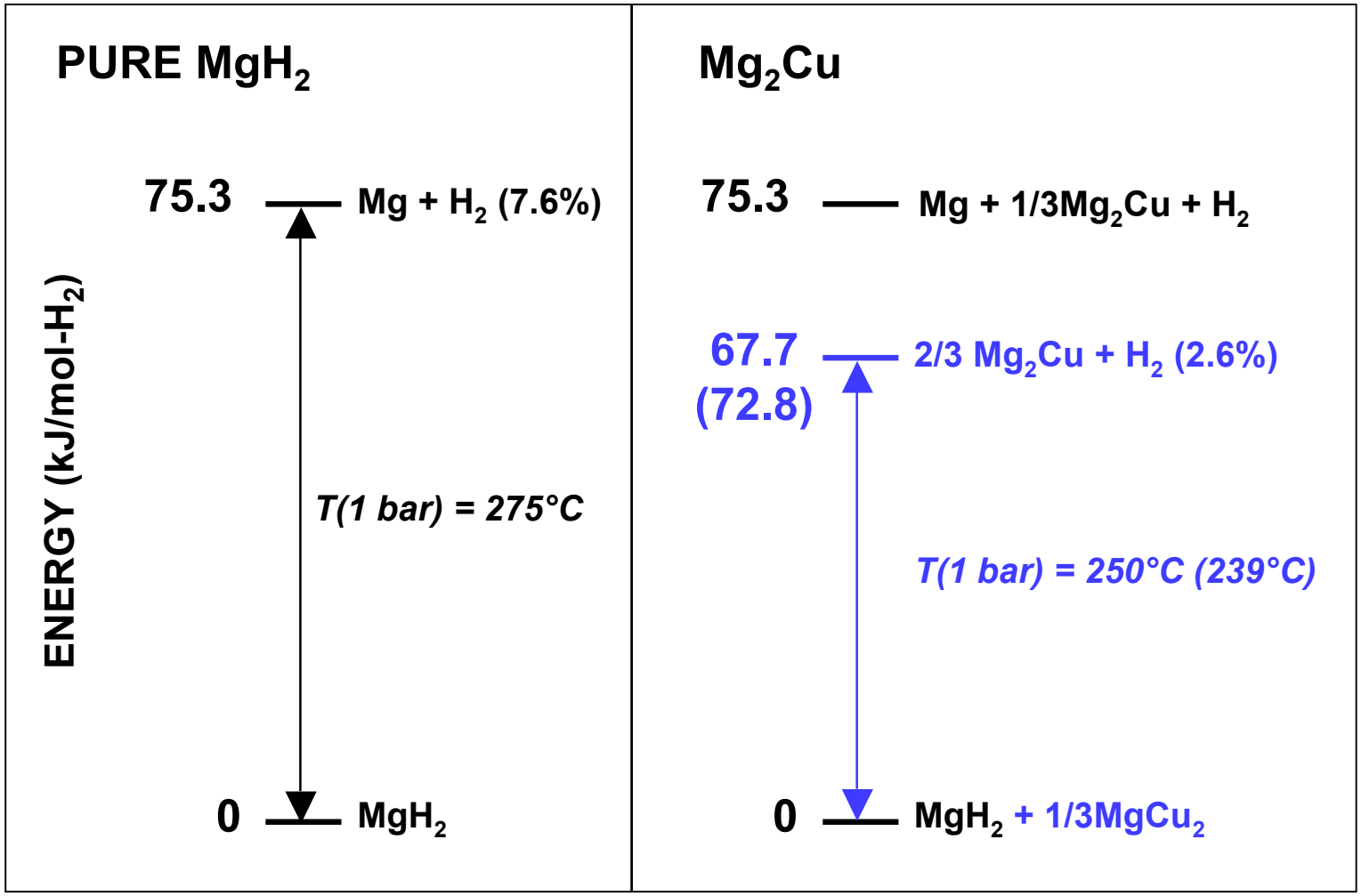

Alloy cohesive energy is small (~ 5 kJ/atom), therefore destabilization is small

** Reilly and Wiswall (1967)*

Destabilization in LiH

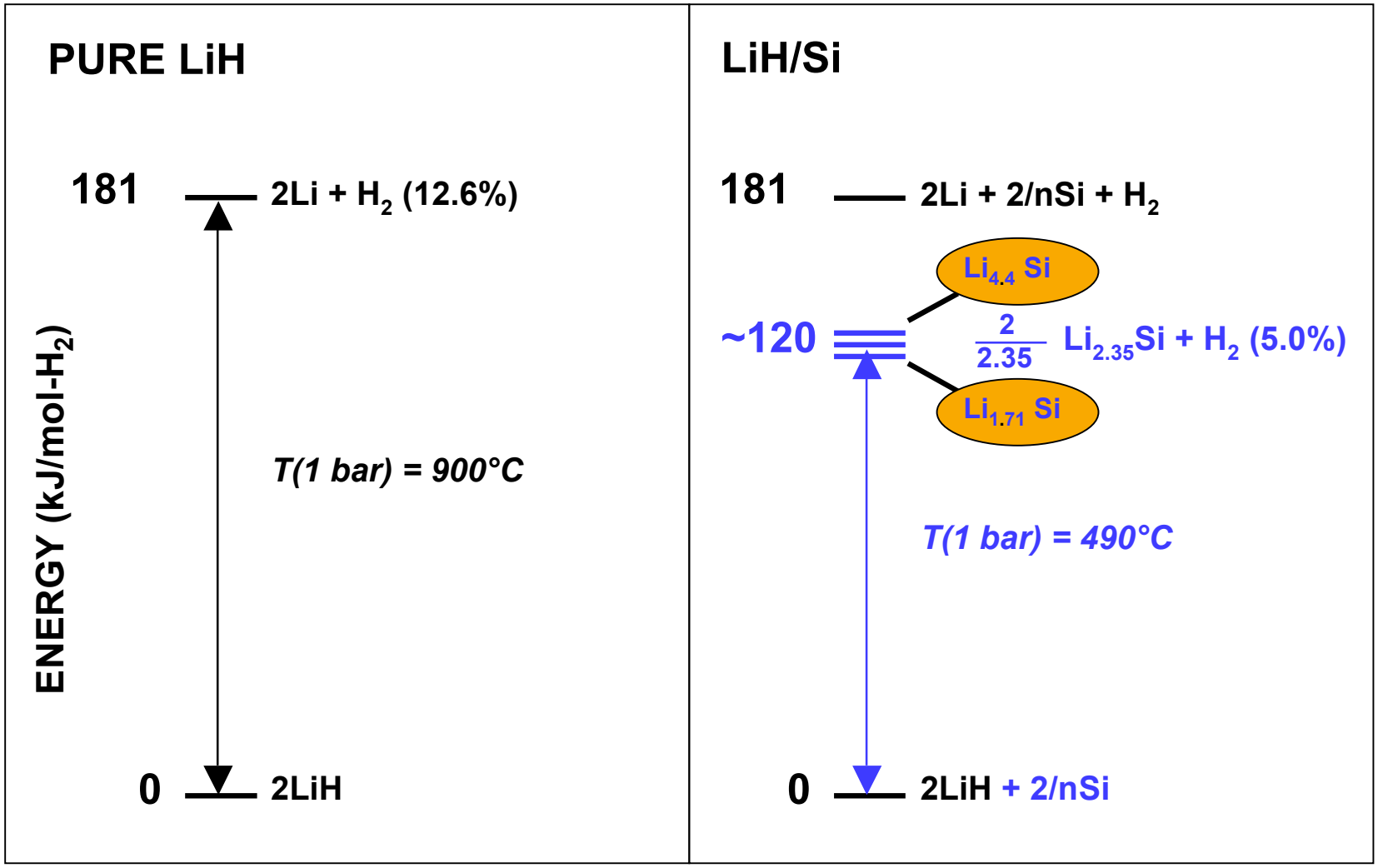

1703-05-00

Cohesive energy of Li_nSi is large (~30 kJ/Li atom) ⇒ destabilization is large

Vajo, J. J. Mertens, F. Ahn, C. C. Bowman, R. C., Jr. Fultz, B., *J. Phys. Chem. B* **2004**, *108*, 13977.

LiH + Si kinetic behavior

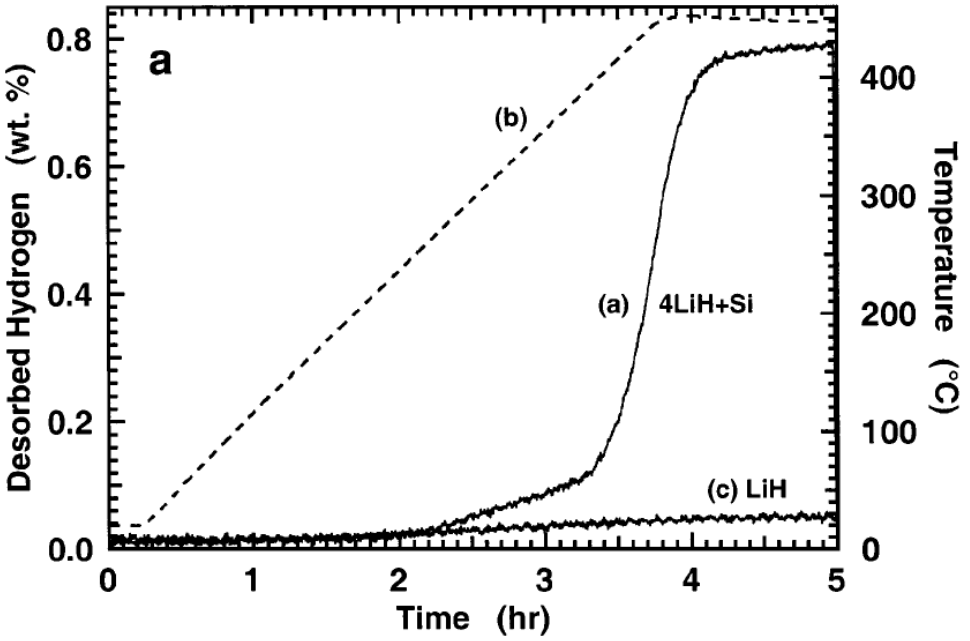

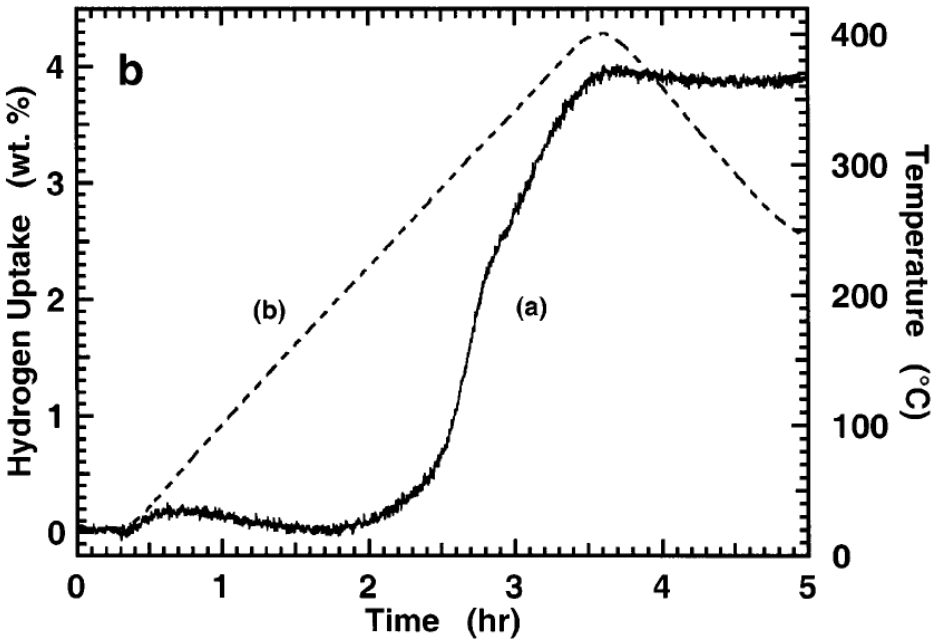

LiH/Si System: Isotherms* for 2.5LiH + Si

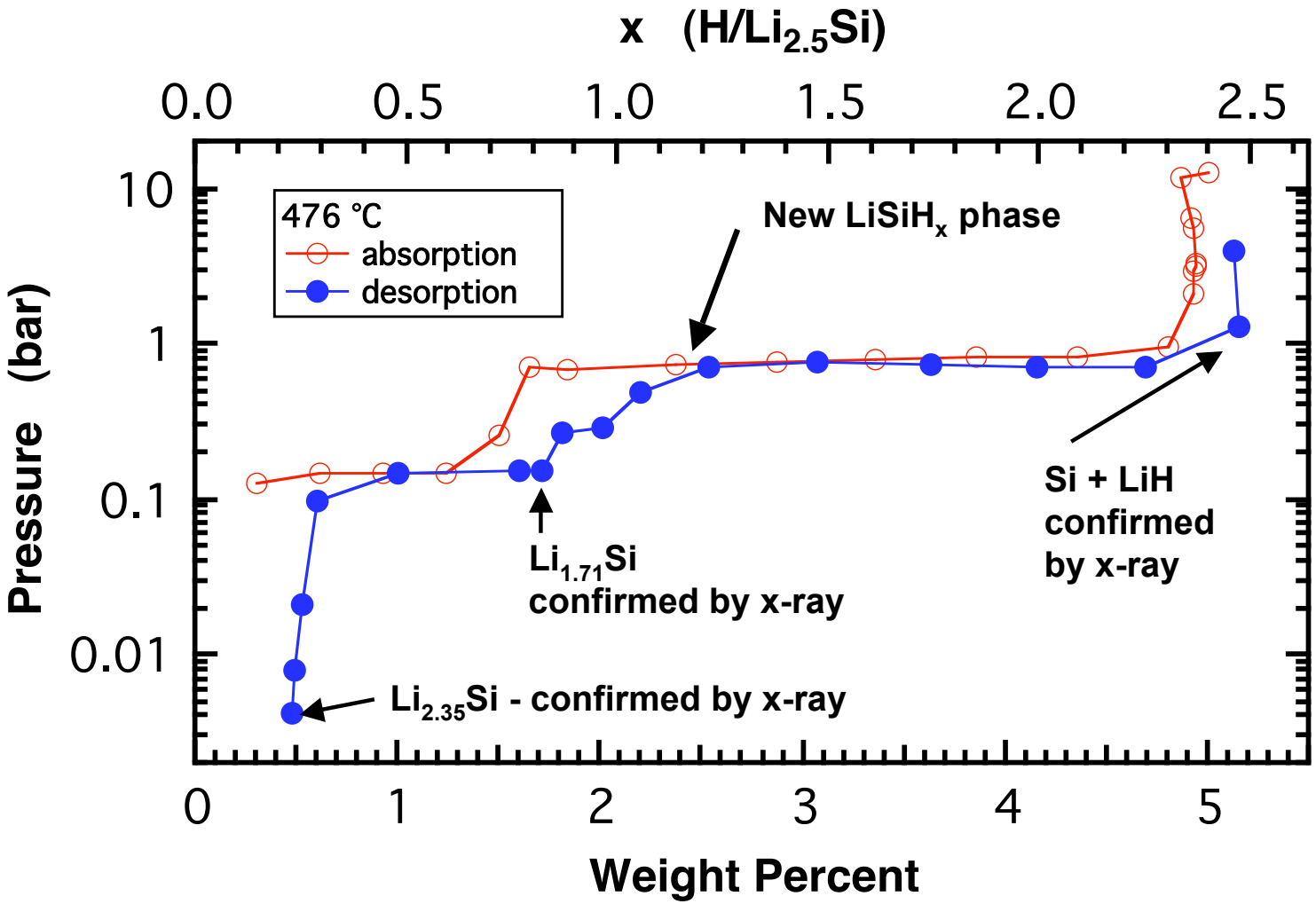

System is reversible; P_{eq} sensitive measure of $\Delta H(Li_nSi)$

** R. C. Bowman, Jr., JPL*

LiH/Si System: van't Hoff Plot

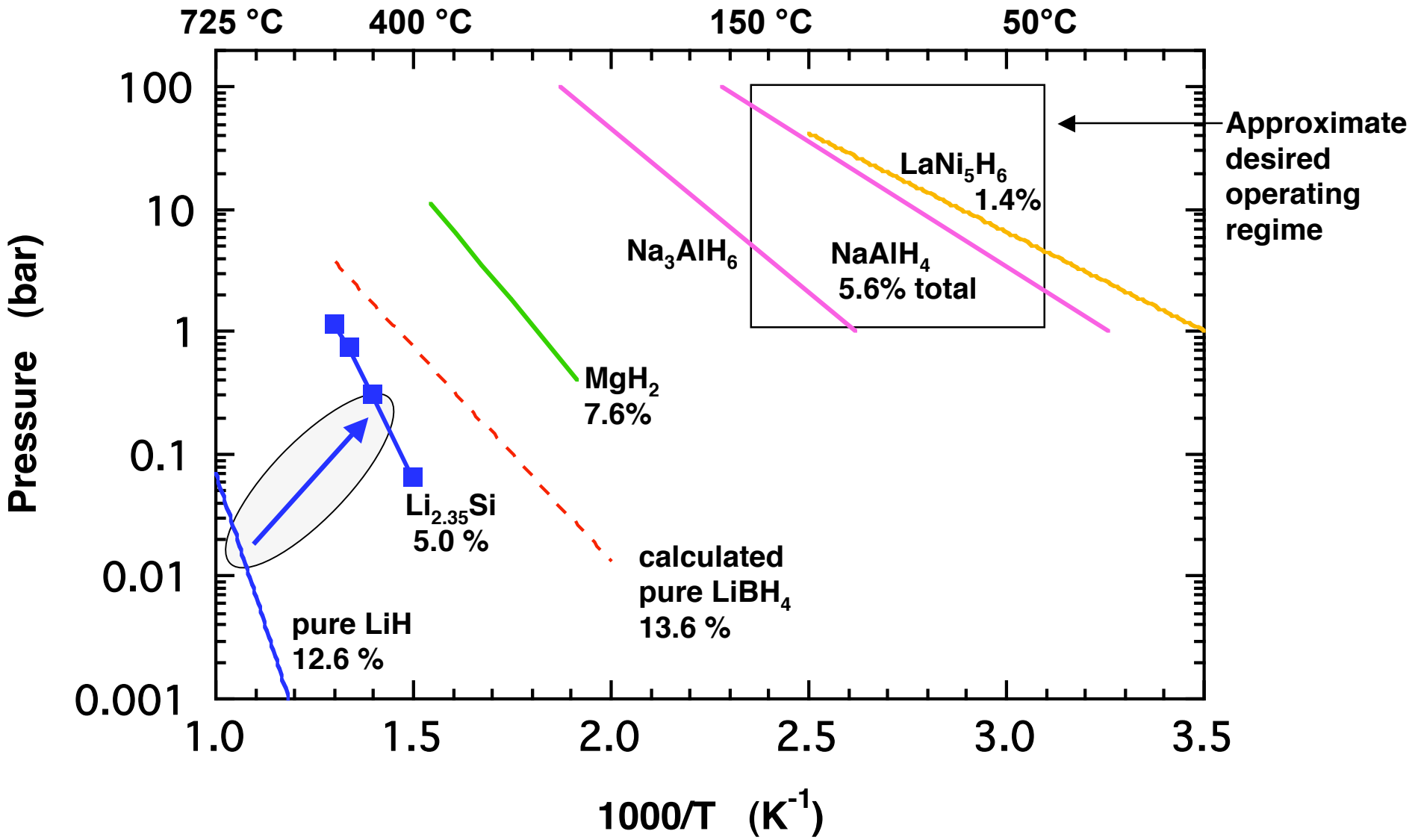

Addition of Si increases P_{eq} by > 10^4 x, decreases ΔH by 60 kJ/mol-H_2

From J. Vajo, HRL Laboratories

Theoretical screening of destabilization reactions

Large-Scale Screening of Metal Hydride Mixtures for High-Capacity Hydrogen Storage from First-Principles Calculations

Alapati, Johnson and Sholl, J. Phys. Chem. C, March 2008.

First-principles calculations have been used to systematically screen >16 million mixtures of metal hydrides and related compounds to find materials with high capacity and favorable thermodynamics for reversible storage of hydrogen. These calculations are based on a library of crystal structures of >200 solid compounds comprised of Al, B, C, Ca, K, Li, Mg, N, Na, Sc, Si, Ti, V, and H. Thermodynamic calculations are used that rigorously describe the reactions available within this large library of compounds. Our calculations extend previous efforts to screen mixtures of this kind by orders of magnitude and, more importantly, identify multiple reactions that are predicted to have favorable properties for reversible hydrogen storage.

TABLE 1: Complete List of Single-Step Reactions Identified from a 212 Compound Database With >6 wt % H_2 Released at Completion and $15 \leq \Delta U_0 \leq 75$ kJ/mol H_2[a]

reaction	wt % H_2	ΔU_0 (kJ/mol H_2)
$Mg(BH_4)_2 \rightarrow MgB_2 + 4H_2$	14.9	54.0
$Si + 4Mg(BH_4)_2 \rightarrow Mg_2Si + 2MgB_4 + 16H_2$	13.2	52.7
$LiBH_4 + C \rightarrow LiBC + 2H_2$	11.9	45.1
$6LiBH_4 + CaH_2 \rightarrow 6LiH + CaB_6 + 10H_2$	11.7	62.1
$8LiBH_4 + MgH_2 + BN \rightarrow 8LiH + MgB_9N + 13H_2$	11.6	66.3
$2LiBH_4 + MgH_2 \rightarrow 2LiH + MgB_2 + 4H_2$	11.5	66.2
$3Si + MgSiN_2 + 12Mg(BH_4)_2 \rightarrow 4Mg_2Si + 2MgB_9N + 36H_2$	11.2	48.6
$BN + 4Mg(BH_4)_2 \rightarrow 3MgH_2 + MgB_9N + 13H_2$	10.9	51.2
$NaH + 2Mg(BH_4)_2 \rightarrow NaMgH_3 + MgB_4 + 7H_2$	10.67	53.2
$CaH_2 + 1.5Si + 3Mg(BH_4)_2 \rightarrow CaB_6 + 1.5Mg_2Si + 13H_2$	10.6	45.4
$2C + Mg(BH_4)_2 \rightarrow MgB_2C_2 + 4H_2$	10.3	43.1
$CaH_2 + 3Mg(BH_4)_2 \rightarrow 3MgH_2 + CaB_6 + 10H_2$	9.9	47.5
$8LiBH_4 + Mg_2Si \rightarrow 8LiH + Si + 2MgB_4 + 12H_2$	9.6	74.0
$2LiBH_4 + ScH_2 \rightarrow 2LiH + ScB_2 + 4H_2$	8.9	49.7
$2LiBH_4 + TiH_2 \rightarrow 2LiH + TiB_2 + 4H_2$	8.6	22.2
$2LiBH_4 + NaMgH_3 \rightarrow 2LiH + NaH + MgB_2 + 4H_2$	8.6	68.9
$3NaH + BN + 4Mg(BH_4)_2 \rightarrow 3NaMgH_3 + MgB_9N + 13H_2$	8.4	48.8
$2LiBH_4 + Mg(NH_2)_2\ MgH_2 + 2LiH + 2BN + 4H_2$	8.1	20.6
$ScH_2 + Mg(BH_4)_2 \rightarrow MgH_2 + ScB_2 + 4H_2$	8.0	37.5
$MgH_2 \rightarrow Mg + H_2$	7.7	64.7
$5B + Mg(BH_4)_2 \rightarrow MgB_7 + 4H_2$	7.5	41.5
$2MgH_2 + Mg(NH_2)_2 \rightarrow Mg_3N_2 + 4H_2$	7.4	26.0
$CaH_2 + 3NaH + 3Mg(BH_4)_2 \rightarrow 3NaMgH_3 + CaB_6 + 10H_2$	7.3	44.3
$6LiBH_4 + 2ScN \rightarrow 6LiH + 2ScB_2 + 2BN + 9H_2$	7.3	59.5
$3Si + 8BN + 5Mg(BH_4)_2 \rightarrow 2MgB_9N + 3MgSiN_2 + 20H_2$	7.3	47.0
$4LiBH_4 + K_2MgH_4 \rightarrow 4LiH + MgB_4 + 2KH + 7H_2$	7.3	74.8
$4LiH + 3Mg(NH_2)_2 + 2C \rightarrow 2Li_2CN_2 + 2Mg_3N_2 + 8H_2$	7.2	47.8
$6LiBH_4 + 2TiN \rightarrow 6LiH + 2TiB_2 + 2BN + 9H_2$	7.1	35.9
$2LiNH_2 + C \rightarrow Li_2CN_2 + 2H_2$	7.0	31.4
$Al + MgB_9N + 2.5Mg(BH_4)_2 \rightarrow AlN + 3.5MgB_4 + 10H_2$	6.8	53.6
$2LiBH_4 + MgB_2 \rightarrow 2LiH + MgB_4 + 3H_2$	6.8	72.5
$MgB_7 + 1.5Mg(BH_4)_2 \rightarrow 2.5MgB_4 + 6H_2$	6.7	50.2
$12LiH + 3Mg(NH_2)_2 + 4BN \rightarrow 4Li_3BN_2 + Mg_3N_2 + 12H_2$	6.7	54.2
$K_2MgH_4 + 2Mg(BH_4)_2 \rightarrow MgB_4 + 2KMgH_3 + 7H_2$	6.6	51.2
$28LiH + 9Mg(NH_2)_2 + 4VN \rightarrow 4Li_7N_4V + 3Mg_3N_2 + 32H_2$	6.5	47.5
$2ScN + 3Mg(BH_4)_2 \rightarrow 3MgH_2 + 2ScB_2 + 2BN + 9H_2$	6.5	43.1
$NaH + ScH_2 + Mg(BH_4)_2 \rightarrow NaMgH_3 + ScB_2 + 4H_2$	6.5	34.8
$4LiBH_4 + 2KMgH_3 \rightarrow 4LiH + MgB_4 + K_2MgH_4 + 7H_2$	6.4	72.2
$2TiN + 3Mg(BH_4)_2 \rightarrow 3MgH_2 + 2TiB_2 + 2BN + 9H_2$	6.4	19.5
$2LiH + LiNH_2 + BN \rightarrow Li_3BN_2 + 2H_2$	6.3	49.1
$2Li_3Na(NH_2)_4 + 4C \rightarrow 3Li_2CN_2 + Na_2CN_2 + 8H_2$	6.1	32.6
$4LiH + 3LiNH_2 + VN \rightarrow Li_7N_4V + 5H_2$	6.1	37.4
$10LiH + 5LiNH_2 + N_4Si_3 \rightarrow 3Li_5N_3Si + 10H_2$	6.0	60.1

The $ScH_2 + 2LiBH_4 \rightarrow ScB_2 + 2LiH + 5/2H_2$ System: *Experimental Assessment of Chemical Destabilization*[a]

- Destabilization reaction with ideal thermodynamic properties (DFT)
  - ΔH_{300K} = 34.1kJ/mol[b]
  - 8.91 wt% capacity
- Isothermal kinetic desorption measurments (450ºC)
  - 4.5 wt% desorption
- Powder XRD detects only LiH and ScH_2 crystalline phases in desorption product, i.e. no reaction under these conditions between ScH_2 and $LiBH_4$.
- Stability of ScH_2, ScB_2 plays critical role in determining overall kinetics.

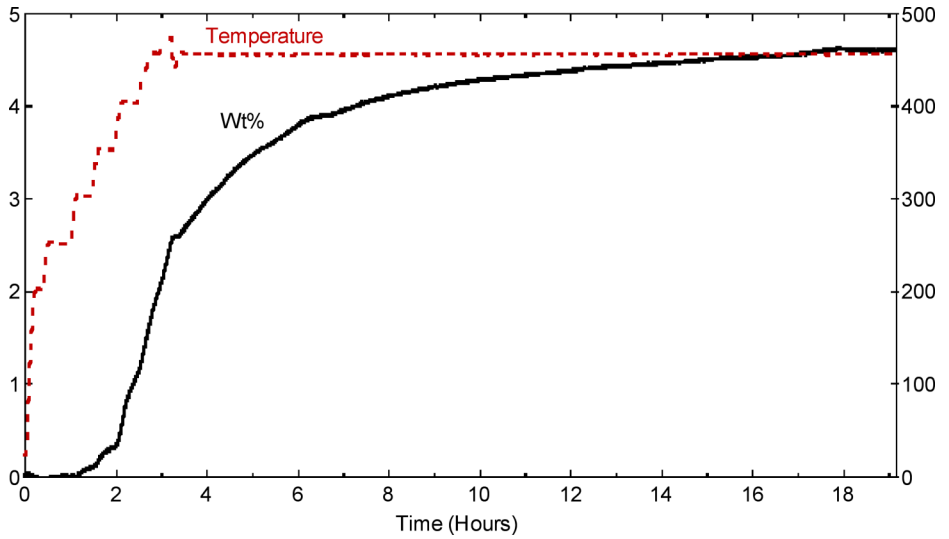

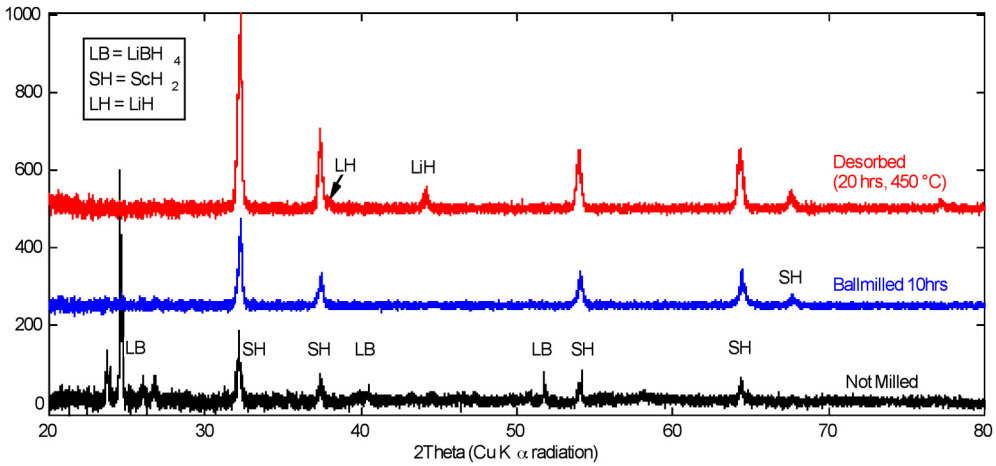

[a]Hydrogen Sorption Behavior of the ScH_2-$LiBH_4$ System: Experimental Assesment of Chemical Destabilization Effects, *Justin Purewal, Son-Jong Hwang, Robert C. Bowman, Jr., Ewa Rönnebro, Brent Fultz and Channing Ahn, accepted for publication in J. Phys. Chem. C (2008).*

[b]Calculated by Center partner David Sholl and published as Alapati, S. V.; Johnson, J. K.; Sholl, D. S., J. Alloys Compd. 2007, 446–447, 23.

The ScH_2+2$LiBH_4$ → ScB_2 + 2LiH + 5/2H_2 System (continued): *MAS-NMR Spectroscopy*

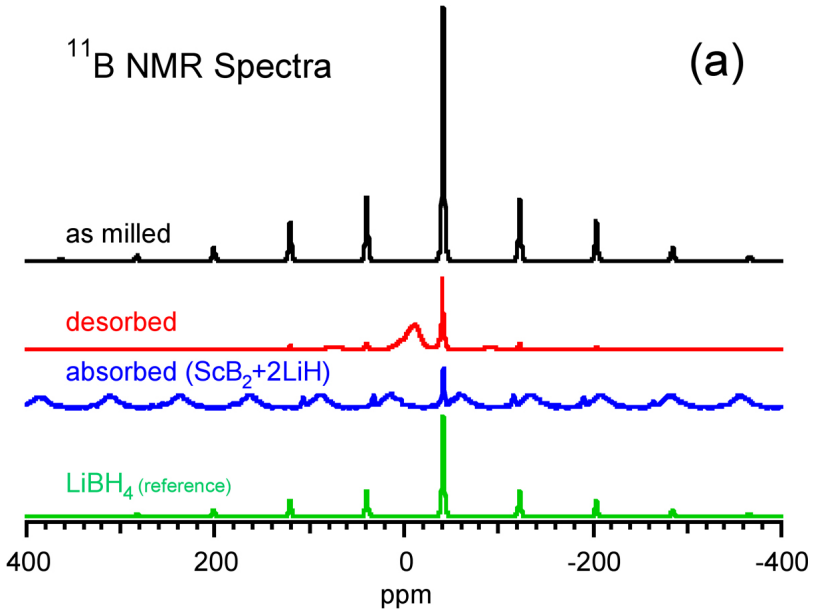

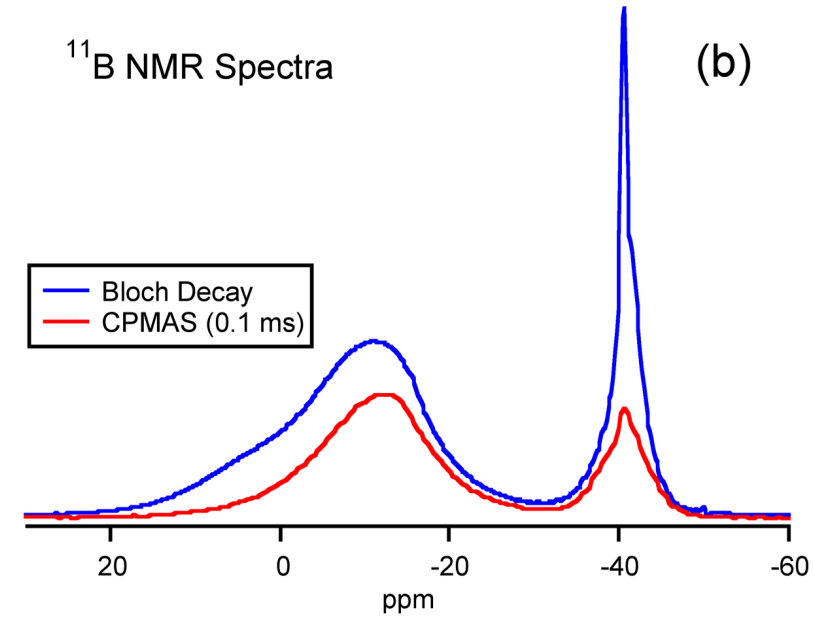

(a) Bloch decay ^{11}B MAS NMR spectra with neat $LiBH_4$ (Sigma-Aldrich) added as a reference. No change of $LiBH_4$ peak observed after ball milling. ^{11}B MAS and CPMAS spectra (a and b) show formation of elemental boron in the amorphous phase (broad shoulder at ~ 5 ppm) and formation of intermediate phase (with peak at -12 ppm), recently identified* as $[B_{12}H_{12}]^{2-}$ species. Note that a ^{11}B MAS NMR spectrum of ScB_2+2LiH system after absorption treatment at high H_2 pressure (896 bar, and 460°C for 48 hr) also included where the broader spinning sidebands in this spectrum are due to un-reacted ScB_2. The small peak at -41 ppm, indicates very limited $LiBH_4$ formation (~ 3%) in the reaction product. So reverse reaction is seen but under technologically challenging conditions.

(b) ^{11}B MAS and CPMAS NMR spectra (contact time=0.1 ms) of desorbed sample.

*NMR Confirmation for Formation of $[B_{12}H_{12}]^{2-}$ Complexes during Hydrogen Desorption from Metal Borohydrides, Son-Jong Hwang, Robert C. Bowman, Jr., Joseph W. Reiter, Job Rijssenbeek, Grigorii L. Soloveichik, Ji-Cheng Zhao, Houria Kabbour, and Channing C. Ahn, J. Phys Chem. C, 112, 3164-3169, 2008.

Solid state diffusion in $ScH_2+2LiBH_4$ => $ScB_2+2LiH+4H_2$

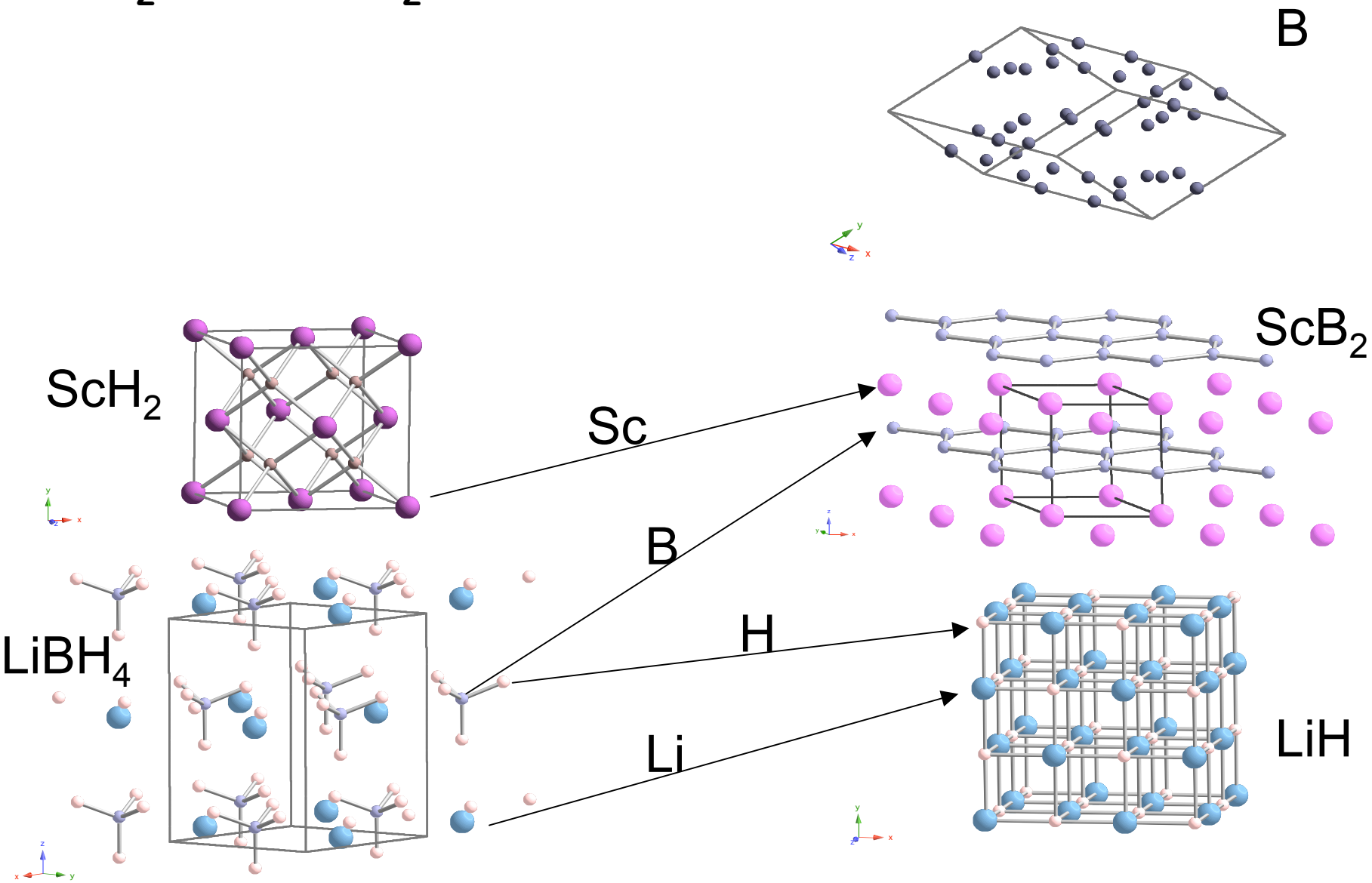

Borohydride analysis: formation of intermediates

NMR Confirmation for Formation of $[B_{12}H_{12}]^{2-}$ Complexes during Hydrogen Desorption from Metal Borohydrides Son-Jong Hwang,*,† Robert C. Bowman, Jr.‡ Joseph W. Reiter,‡ Job Rijssenbeek,§ Grigorii L. Soloveichik,§ Ji-Cheng Zhao,§ Houria Kabbour,| and Channing C. Ahn, J. Phys Chem. C. (2008).

^{11}B NMR spectroscopy has been employed to identify the reaction intermediates and products formed in the amorphous phase during the thermal hydrogen desorption of metal tetrahydroborates (borohydrides) $LiBH_4$, $Mg(BH_4)_2$, $LiSc(BH_4)_4$, and the mixed $Ca(AlH_4)2$-$LiBH_4$ system. The ^{11}B magic angle spinning (MAS) and cross polarization magic angle spinning (CPMAS) spectral features of the amorphous intermediate species closely coincide with those of a model compound, closo-borane $K_2B_{12}H_{12}$ that contains the $[B_{12}H_{12}]^{2-}$ anion. The presence of $[B_{12}H_{12}]^{2-}$ in the partially decomposed borohydrides was further confirmed by high-resolution solution ^{11}B and ^{1}H NMR spectra after dissolution of the intermediate desorption powders in water. The formation of the closo-borane structure is observed as a major intermediate species in all of the metal borohydride systems we have examined.

Assumed dehydrogenation reactions:

$M(BH4)_n \rightarrow M + nB + (2n)H_2$

$M(BH4)_n \rightarrow MH_x + nB + [2n-x/2]H_2$

But, formation of $M_{2/n}B_{12}H_{12}$ phases as major intermediate species as determined by NMR

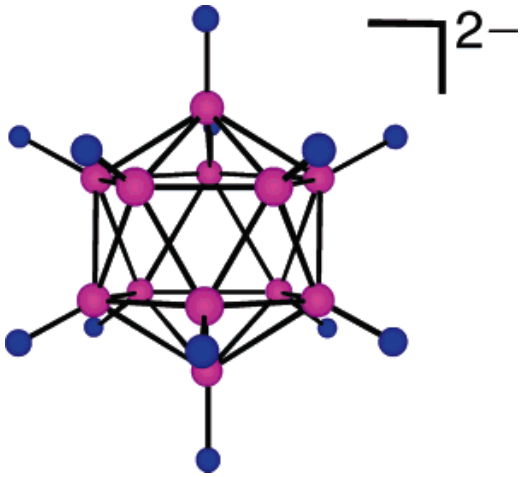

Summary of hydride and destabilization reactions

- Equilibrium thermodynamic evaluation a critical starting point in determining absorbents of engineering value.
- Awareness of constituent formation enthalpies may also be an important consideration for work where destabilization reaction enthalpies used for materials assessment.
- Reaction pathways not always predictable.

Acknowledgements:

Anne Dailly, now at GM
Angelique Saulnier, now at Samsung
Houria Kabbour, now at CNRS

John Vajo, HRL Laboratories
R. C. Bowman Jr., JPL (consulting to DoE)
Joe Reiter and Jason Zan, JPL
Sonjong Hwang, Caltech Solid State NMR facility

Justin Purewal
Nick Stadie
David Abrecht

Ted Baumann, LLNL

Support through: Energy Efficiency and Renewable Energy at DoE,
Ned Stetson and Carole Read
GM, Scott Jorgensen and Jim Spearot

Sieverts apparatus

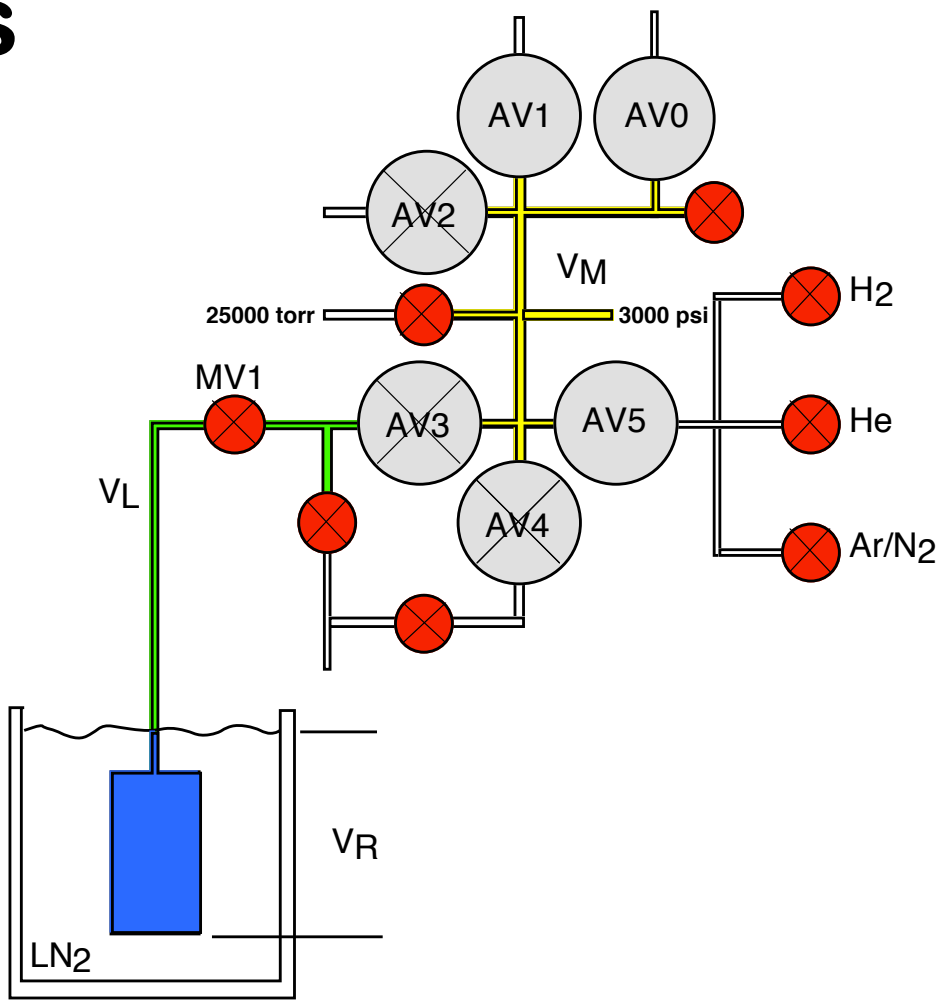

Pressurize manifold by pressurizing line before AV5.
Open AV5. Wait for equilibration (almost instantaneous).
Record pressure (from PR4000 and divide by 4) and manifold temperature (from panel readout).
Open AV3. Wait for equilibration (almost instantaneous).
Record pressure (from PR4000 and divide by 4) and manifold temperature (from panel readout).
Open manual valve to sample. Wait for equilibration (5 min. should be enough).
Record pressure (from PR4000 and divide by 4) and manifold temperature (from panel readout).

Isotherms from metal organic frameworks

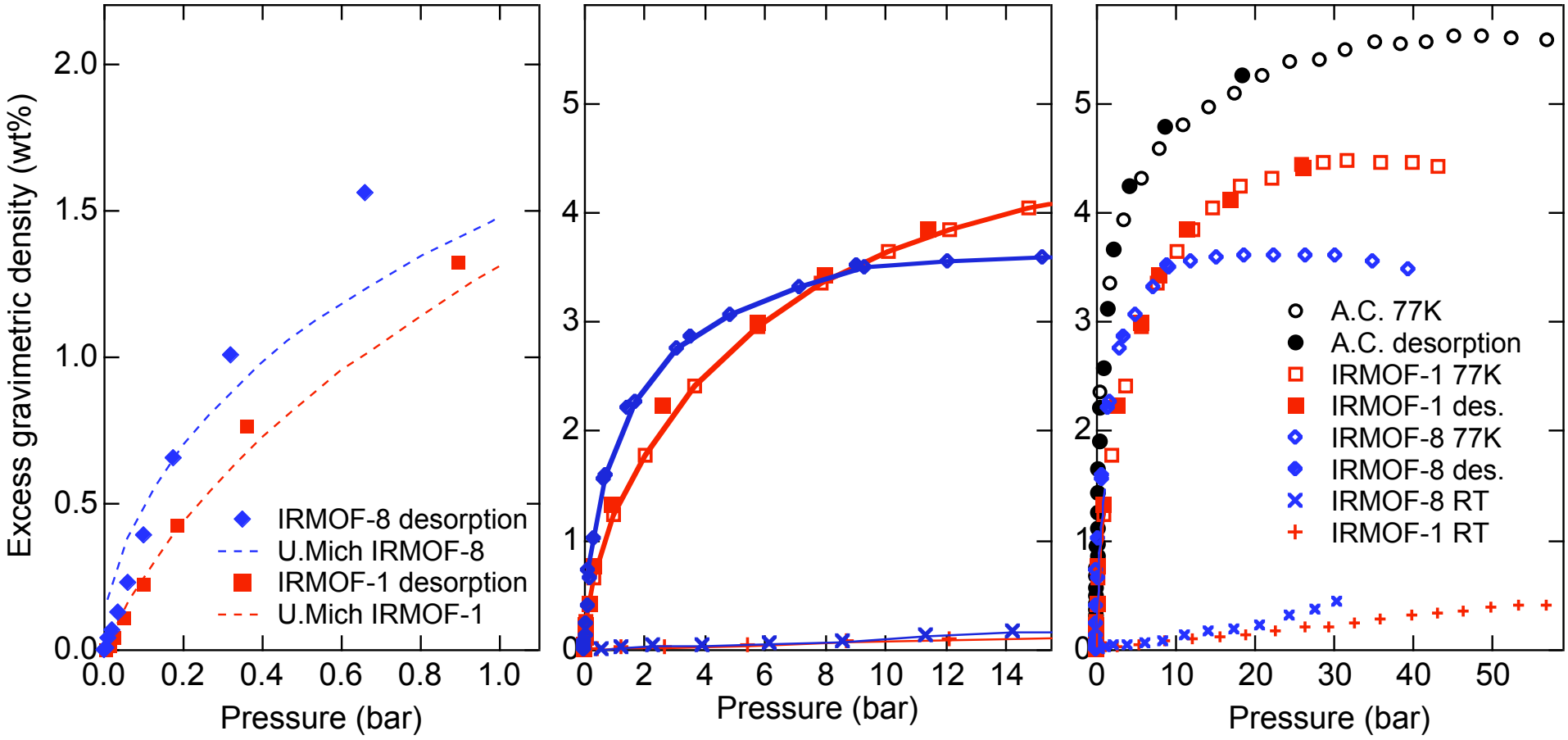

Low pressure data to 1 bar not a predictor of saturation behavior, only an indication of sorption heat (high slope => higher heat, IRMOF-1 ~4kJ/mole, IRMOF-8 ~6kJ/mole). Activated carbon sample from F. Baker and N. Gallego, ORNL.

A. Dailly, J. J. Vajo and C. C. Ahn, J. Phys. Chem B, v110, p1099, (2006)